

***Arabidopsis* Small Ubiquitin-Like Modifier Paralogs Have Distinct Functions in Development and Defense**

Harrold A. van den Burg,^{a,b,c} Ramachandra K. Kini,^{a,1} Robert C. Schuurink,^d and Frank L.W. Takken^{a,2}

^a Plant Pathology, Swammerdam Institute for Life Sciences, University of Amsterdam, 1098 XH Amsterdam, The Netherlands

^b Laboratory for Phytopathology, Wageningen University, 6708 PB, Wageningen, The Netherlands

^c Centre for BioSystems Genomics, 6700 AB, Wageningen, The Netherlands

^d Plant Physiology, Swammerdam Institute for Life Sciences, University of Amsterdam, 1098 XH Amsterdam, The Netherlands

Posttranslational modifications allow dynamic and reversible changes to protein function. In *Arabidopsis thaliana*, a small gene family encodes paralogs of the small ubiquitin-like posttranslational modifier. We studied the function of these paralogs. Single mutants of the *SUM1* and *SUM2* paralogs do not exhibit a clear phenotype. However, the corresponding double knockdown mutant revealed that *SUM1* and *SUM2* are essential for plant development, floral transition, and suppression of salicylic acid (SA)-dependent defense responses. The *SUM1* and *SUM2* genes are constitutively expressed, but their spatial expression patterns do not overlap. Tight transcriptional regulation of these two *SUM* genes appears to be important, as overexpression of either wild-type or conjugation-deficient mutants resulted in activation of SA-dependent defense responses, as did the *sum1 sum2* knockdown mutant. Interestingly, expression of the paralog *SUM3* is strongly and widely induced by SA and by the defense elicitor Flg22, whereas its expression is otherwise low and restricted to a few specific cell types. Loss of *SUM3* does not result in an aberrant developmental phenotype except for late flowering, while *SUM3* overexpression causes early flowering and activates plant defense. Apparently, *SUM3* promotes plant defense downstream of SA, while *SUM1* and *SUM2* together prevent SA accumulation in noninfected plants.

INTRODUCTION

Posttranslational modifications (PTMs) set a reversible mark on specific amino acids, enabling proteins to change conformation or to recruit and interact with specific partners. These PTM-induced interactions allow, for example, dynamic responses to stress conditions or determine developmental patterns in higher eukaryotes. A prominent member of the Ubiquitin-like class of PTMs is SMALL UBIQUITIN-LIKE MODIFIER (SUMO) (Downes and Vierstra, 2005). In budding yeast (*Saccharomyces cerevisiae*) and humans, SUMO protein modifications are well characterized and linked to nuclear processes, such as nuclear import, transcription, chromatin remodeling, and DNA replication (Heun, 2007). It has become clear that in plants these nuclear processes are also regulated by SUMO, despite the fact that only a small number of plant SUMO targets have been identified (Miura et al., 2005, 2007b; Garcia-Dominguez et al., 2008; Jin et al., 2008; Budhiraja et al., 2009). Some eukaryotes (e.g., yeast [*S. cerevi-*

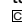
siae], flies [*Drosophila melanogaster*], and worms [*Caenorhabditis elegans*]) express only a single SUMO gene, whereas vertebrates express up to four paralogs. The genome of the model plant *Arabidopsis thaliana* potentially encodes eight SUMO paralogs (Kurepa et al., 2003; Novatchkova et al., 2004). Currently, only four of these (SUM1, SUM2, SUM3, and SUM5) have been shown to act as functional PTMs (Colby et al., 2006; Budhiraja et al., 2009). SUM1 and SUM2 are most closely related, sharing 89% protein sequence identity, whereas SUM3 shows 48% identity and SUM5 only 35% identity to SUM1. These sequence differences suggest functional diversification of these paralogs.

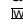
The process of SUMO conjugation is largely conserved among yeast, mammals, and plants. First, SUMO precursors undergo C-terminal processing by SUMO proteases (also referred to as Ubiquitin-like proteases or Ulp) that liberate a C-terminal double-Gly motif. Subsequently, this mature form of SUMO is conjugated to target proteins via two consecutive steps catalyzed by the SUMO E1 ACTIVATING ENZYME (SAE1/SAE2 in *Arabidopsis*) and the SUMO E2 CONJUGATING ENZYME (SCE1 in *Arabidopsis*; Ubc9 in yeast and mammals). SUMO conjugation (called SUMOylation) results in the formation of an isopeptide bond between the SUMO C terminus and the side chain of an acceptor Lys in target proteins. SUMOylation is essential in *Arabidopsis* (i.e., null mutants of SAE1/SAE2 and SCE1 are embryo lethal) (Saracco et al., 2007). SCE1 can directly recognize and SUMOylate Lys residues embedded in a SUMOylation consensus motif (Ψ -K-X-E/D, where Ψ denotes a bulky hydrophobic residue and X any residue). SCE1-mediated SUMOylation can be promoted by SUMO E3 ligases (Bernier-Villamor et al., 2002; Yunus and Lima, 2006; Anckar and Sistonen,

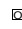
¹ Current address: Department of Studies in Biotechnology, University of Mysore, Manasagangotri, Mysore 570 006, India.

² Address correspondence to f.l.w.takken@uva.nl.

The authors responsible for distribution of materials integral to the findings presented in this article in accordance with the policy described in the Instructions for Authors (www.plantcell.org) are: Harrold A. van den Burg (harrold.vandenburg@wur.nl) and Frank L.W. Takken (f.l.w.takken@uva.nl).

 Some figures in this article are displayed in color online but in black and white in the print edition.

 Online version contains Web-only data.

 Open Access articles can be viewed online without a subscription. www.plantcell.org/cgi/doi/10.1105/tpc.109.070961

2007). Loss of the *Arabidopsis* SUMO E3 ligase HIGH PLOIDY2 (HPY2) leads to severe dwarfism, and HPY2 was found to be essential for proper meristem development (Huang et al., 2009; Ishida et al., 2009). Loss of the *Arabidopsis* SUMO E3 ligase SAP AND MIZ1 (SIZ1) results in dwarfism, early flowering, altered responses to abiotic stresses (salt, cold, and drought and the plant hormone abscisic acid), and induction of salicylic acid (SA)-dependent disease resistance responses (Miura et al., 2005, 2007b, 2009, 2010; Yoo et al., 2006; Catala et al., 2007; Lee et al., 2007; Jin et al., 2008; Cheong et al., 2009).

SUMOylation is reversible, and deconjugation is catalyzed by SUMO proteases. Plant SUMO proteases appear to have redundant and nonredundant functions, as exemplified by distinct phenotypes for different knockout mutants. For instance, EARLY IN SHORT DAYS4 (ESD4/Ulp1b) is essential for normal plant development (Reeves et al., 2002; Murtas et al., 2003). By contrast, OVERLY TOLERANT TO SALT1 and 2 (OTS1/Ulp1d and OTS2/Ulp1c) act redundantly in salt tolerance without exhibiting aberrant developmental phenotypes for the *ots1 ots2* double mutant (Conti et al., 2008). These different biological functions can in part be explained by different biochemical activities toward SUMO paralogs and a discrete distribution of these proteases in the nucleus. For instance, OTS1, OTS2, and ESD4 each displayed different (iso)peptidase activities toward SUM1 and SUM2 conjugated proteins (Chosed et al., 2006). In addition, ESD4 was found to localize to the nuclear rim, while OTS1 and OTS2 localized to the nucleoplasm and predominantly to nuclear bodies, respectively (Murtas et al., 2003; Xu et al., 2007; Conti et al., 2008).

A substantial number of SUMO targets are SUMOylated at nonconsensus sites via a mechanism that involves noncovalent interactions between SUMO and the SUMO interaction motif (SIM) (Zhu et al., 2008; Blomster et al., 2009). In mammals, these SUMO–SIM interactions are paralog specific and determine recruitment of Ubc9 (E2) to certain SUMO targets, implying that SUMO–SIM interactions have a role in paralog-specific SUMOylation (Hecker et al., 2006; Ghisletti et al., 2007; Knipscheer et al., 2008; Meulmeester et al., 2008). Moreover, SUMO–SIM interactions determine the subnuclear distribution of SUMO-modified proteins, confer paralog-specific protection against isopeptidase activity, and promote paralog-specific recruitment of downstream-acting proteins (Yamaguchi et al., 2005; Ihara et al., 2007; Zhu et al., 2008, 2009; Blomster et al., 2009). These observations demonstrate that mammalian SUMO paralogs have acquired distinct biological functions.

Phylogenetic analysis indicates that the SUMO gene family has independently expanded in mammals and plants and, like in mammals, plant paralogs appear to have acquired distinct properties (Colby et al., 2006). For instance, SUM1 and SUM2 can form poly-SUMO chains, whereas SUM3 lacks an internal SUMOylation motif required for chain formation (Colby et al., 2006; Budhiraja et al., 2009). Furthermore, several *Arabidopsis* SUMO proteases exhibit low isopeptidase activity toward SUM3-conjugated proteins but show high activity toward SUM1 and SUM2 conjugates (Chosed et al., 2006; Colby et al., 2006).

We examined the different biological functions of the *Arabidopsis* SUMO paralogs. The functions of these proteins are

poorly understood due to the absence of a *sum3* null mutant, embryonic lethality of the *sum1 sum2* double mutants, and lack of phenotypes for the single *sum1* and *sum2* mutants (Saracco et al., 2007). Here, we report a viable *sum1 sum2* knockdown mutant and a *sum3* knockout mutant in *Arabidopsis*. Our data suggest that SUM3 acts downstream of SA accumulation, while SUM1 and SUM2 are involved in suppressing SA accumulation. Apparently, the *Arabidopsis* SUMO paralogs form a regulatory network that differentially modulates innate immune responses and flowering time.

RESULTS

Arabidopsis SUMO Paralogs Exhibit Distinct Gene Expression Patterns

To study the spatial and development expression patterns of the *Arabidopsis* SUMO paralogs, we isolated the promoters of the SUM genes and fused them to the β -glucuronidase (GUS) reporter gene. We focused our studies on the *Arabidopsis* SUM1, SUM2, and SUM3 paralogs, as they form a single phylogenetic clade with other plant homologs, while SUM5 falls outside this clade and has not yet been found in other plant species (see Supplemental Figure 1 and Supplemental Data Set 1 online). GUS staining of the transgenic plants revealed that SUM1 is abundantly and widely expressed in leaf and root tissues, except for in the vasculature, the lateral root primordia, and the root apex (Figure 1). Expression of SUM2 complemented the expression pattern of SUM1 in that expression of SUM2 was high in leaf vasculature, lateral root primordia, and the root apex, while modest in mesophyll cells. The root-specific expression patterns of SUM1 and SUM2 agree with expression data for seedling root cells retrieved from the Bio-Array Resource (BAR) for plant functional genomics (Birnbaum et al., 2003; Brady et al., 2007; Winter et al., 2007).

SUM3 showed a highly tissue-specific expression pattern, as GUS staining was observed only in the hydathodes and leaf vasculature of mature leaves (Figure 1). Hence, SUM3 expression partially overlaps with SUM2 expression in mature leaves. In roots, expression of SUM3 was restricted to specific cell types of the root vasculature and root primordia. The expression patterns of SUM3 in roots correlates with the data present in BAR. In developing flowers, SUM1 expression was observed at the base of the mature flower, in premature anthers, the stigma, and during embryogenesis in developing seeds but not in siliques. SUM2 expression was found in the vasculature of both filaments and sepals, but not petals. Furthermore, expression of SUM2 was seen at the junction of the silique and pedicel, in developing anthers, and in the style. Finally, SUM3 expression appears not to overlap with SUM1 and SUM2 expression patterns in developing flowers (i.e., SUM3 appears to be expressed exclusively in mature pollen and in developing ovaries).

We also noted that SUM1 was expressed throughout all stages of embryonic development (globule, heart, and torpedo stage) (see Supplemental Figure 2 online), while SUM2 was only expressed until the late heart stage of developing embryos. Expression of SUM3 was not detectable in seeds or in embryos. We

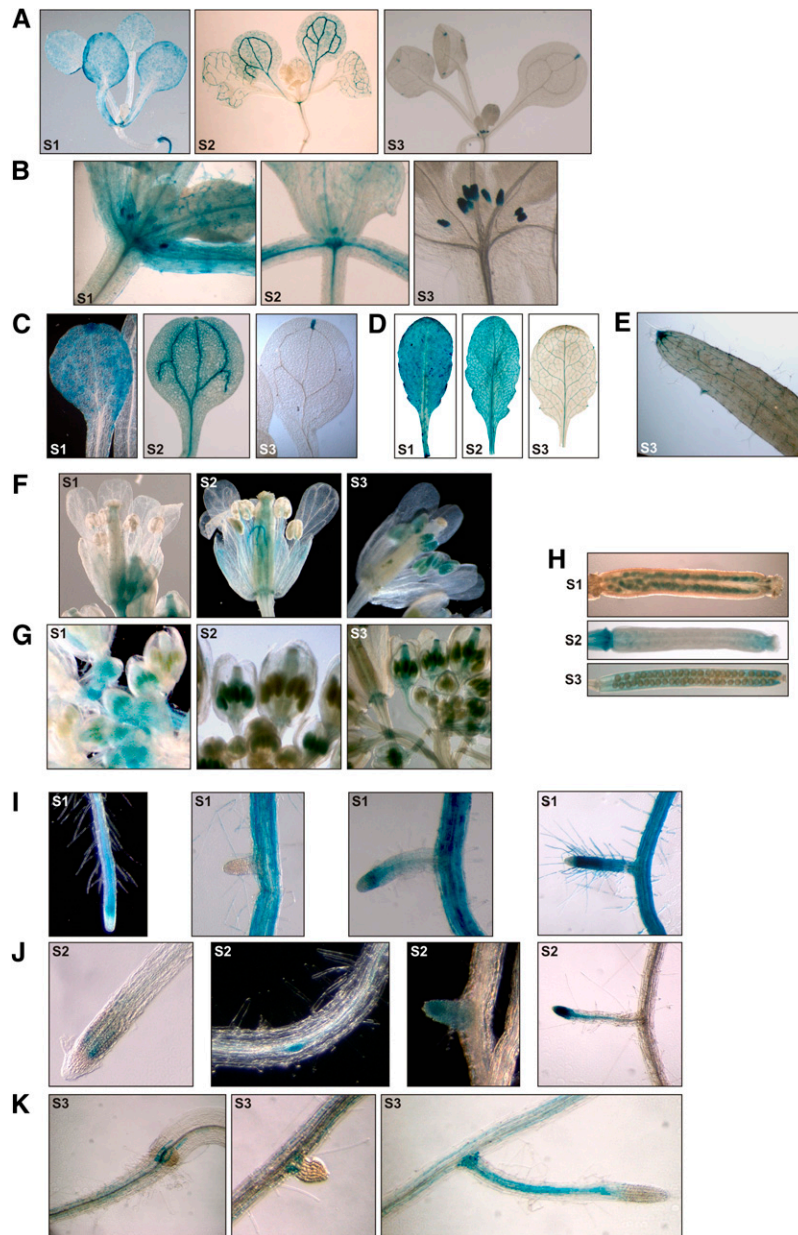


Figure 1. Expression Patterns of the **SUM1**, **SUM2**, and **SUM3** Genes.

Localization of GUS reporter activity in *Arabidopsis* plants transformed with *SUMO* promoter-GUS reporter gene fusions (S1, *ProSUM1-GUS*; S2, *ProSUM2-GUS*; and S3, *ProSUM3-GUS*). GUS localizations were examined in leaf tissue ([A] to [E]), floral development ([F] and [G]), siliques ([H]), and roots ([I] to [K]). At least four independent transgenic lines were examined per construct.

noted that deposited microarray expression data (BAR) for *Arabidopsis* embryogenesis fully supported our observations of expression patterns of these *SUM* genes (Casson et al., 2005; Winter et al., 2007). The expression profiles of *SUM1* and *SUM2* are consistent with their essential role in embryogenesis (Saracco et al., 2007). Overall, these promoter-GUS studies revealed that the *SUM* genes have unique and largely nonoverlapping expression patterns, with *SUM1* and *SUM2* being widely and abundantly expressed.

The SUMO Paralogs Have Distinct Functions in Plant Development

To study the biological function of these *SUMO* genes, we first isolated a null allele (*sum3-1*) of *SUM3* from a suppressor-mutator transposon insertion collection (Tissier et al., 1999) (Figure 2A). Sequencing located the transposon insertion in the third exon, 500 bp downstream of the start codon, where it disrupted the coding sequence of the mature protein (at Met-78). Loss of

SUM1, *SUM2*, and *SUM3* expression in the respective homozygous *sum1-1*, *sum2-1*, and *sum3-1* plants was confirmed by RT-PCR (Figure 2B). Homozygous *sum3-1* plants showed normal plant development, as previously reported for the single *sum1* and *sum2* mutants (Saracco et al., 2007). When we compared the time of bolting (flowering) for individual *SUM* knockout lines under short-day (SD) and long-day (LD) conditions, we observed that under SDs, *sum3-1* was significantly late flowering (Table 1).

As the *sum1 sum2* double null mutant is embryo lethal (Saracco et al., 2007), the combined function of these two paralogs could not be studied in adult plants. To overcome this embryo lethality, we created a *SUM2* knockdown mutant using artificial miRNA (*amiR*) gene silencing (Schwab et al., 2006). The *amiR-SUM2* construct was designed to target the *SUM2* transcript region that encodes the C-terminal tail extension that is removed by SUMO maturation (Figure 2C). We identified several transgenic lines with reduced *SUM2* mRNA levels (97 to 98% reduction) (Figure 2D). These lines did not show substantially altered expression of *SUM1* or *SUM3*, which means that *amiR-SUM2* specifically targets *SUM2* mRNA. None of the independent *amiR-SUM2* lines showed any aberrant developmental defects, analogous to the *sum2-1* null allele. Expression of *amiR-SUM2* is controlled by the 35S cauliflower mosaic virus promoter, which is not expressed until the torpedo stage in plant embryos (Custers et al., 1999; Sunilkumar et al., 2002). Hence, *SUM2* will not be silenced by the *amiR-SUM2* construct during early embryonic development, and, based on its expression profile, this is predicted to allow embryo rescue when the *amiR-SUM2* is introgressed in *sum1-1*. Indeed, we obtained viable homozygous F2 progeny for two independent crosses between *amiR-SUM2* lines and *sum1-1*.

To confirm reduced accumulation of the *SUM2* protein in the *sum1-1 amiR-SUM2* progeny, a heat shock treatment was applied and the free and conjugated *SUM1/2* protein levels were analyzed using immunoblotting (Figure 2E). Heat shock treatment of the parental lines (*sum1-1* and *amiR-SUM2*) resulted in an increase in *SUM1/2* conjugation, as described previously (Saracco et al., 2007). Heat shock treatment of the *sum1-1 amiR-SUM2* seedlings, however, resulted only in a minor increase in *SUM1/2* conjugation levels, while the free *SUM1/2* levels remained below the detection limit. Hence, the double knockdown mutant exhibits strong reduction of *SUM1* and *SUM2* conjugation. In addition, we noted that the double mutant showed increased *SUM3* protein levels (Figure 2F). The *sum1-1 amiR-SUM2* double mutant was partially sterile and displayed a strong developmental phenotype (dominant for the *amiR-SUM2* allele, recessive for the *sum1-1* allele) including dwarfism, shortened petiole length, crooked and asymmetric leaves, leaf fusion, disturbed inflorescence internode patterning and node development, early senescence, and early flowering under both SD and LD conditions (Figures 2G to 2I, Table 1). Clearly, *SUM1* and *SUM2* not only act redundantly during embryogenesis, but together regulate many aspects of plant development. *SUM3* does not have an apparent function in development but is involved in early flowering under SDs (Table 1).

Accumulation of Conjugation-Deficient *SUM1* and *SUM2* Mutants Mimics a *siz1* Phenotype

To further investigate the extent to which the SUMO paralogs affect different biological processes, we created transgenic *Arabidopsis* lines that overexpress either a mature (wild type [WT]) SUMO or a conjugation-deficient mutant (Δ GG) of each paralog. For *SUM1*(WT) and *SUM2*(WT), we identified several highly expressing *Arabidopsis* lines, as evidenced by the high levels of free (nonconjugated) tagged SUMO in the total protein extracts (Figure 3A, α AtSUM1/2- and α HIS-specific antibodies). These lines showed increased accumulation of a high molecular weight (HMW) smear representing SUMOylated proteins. Tagged *SUM1* and *SUM2* are present in this HMW smear as they coprecipitated with the HIS-tagged protein fraction under protein denaturing conditions (6 M GuCl) (Figure 3A, *IP:NI2+*). The HMW smear was SUMO protease sensitive, as in the absence of the SUMO protease inhibitor *N*-ethylmaleimide (NEM) (Lois et al., 2003; Murtas et al., 2003) it partially disappeared and the protein levels of free *SUM1/2* increased (see Supplemental Figure 3 online). To further show that the tagged *SUMO*(WT) proteins are conjugated to SUMO targets in planta, we induced mass SUMOylation using heat shock treatment. After heat shock, the tagged mature *SUM1*, *SUM2*, and *SUM3* proteins were conjugated to other proteins and the SUMOylation levels exceeded those observed in the nontransgenic controls (Figure 3B). This observation implies that in wild-type plants, the levels of free SUMO protein are limiting during the mass SUMOylation triggered by a heat shock.

We also generated transgenic plants that overexpress the conjugation-deficient mutants (Δ GG) of *SUM1*, *SUM2*, or *SUM3*. Surprisingly, high expressors of *SUM1*(Δ GG) and *SUM2*(Δ GG) also showed increased *SUM1/2* conjugation levels (Figure 3A, total protein extract). This indicates that their overexpression either inhibits SUMO deconjugation and/or stimulates SUMO conjugation, as the HMW smear did not coprecipitate with the His-tagged protein fraction in plants expressing the Δ GG mutant (Figure 3A, *IP:NI2+*). Affinity precipitation confirmed that the Δ GG mutants are not conjugated to SUMO targets. Notably, pull-down of *SUM1*(Δ GG) or *SUM2*(Δ GG) revealed an additional protein (complex) of \sim 31 to 35 kD, which we also detected when precipitating *SUM1*(WT) or *SUM2*(WT) (Figure 3A, *IP:NI2+*, 2x*SUM1/2*). As *SUM1* and *SUM2* can form poly-SUMO chains via an internal SUMOylation site (Colby et al., 2006), this larger protein (complex) likely signifies SUMOylation of the Δ GG mutant by endogenous *SUM1* or 2, resulting in SUMO dimers. *SUM3* does not contain an internal SUMOylation site, and, in agreement with this, we did not observe a SUMO dimer when we precipitated tagged *SUM3*(Δ GG) (neither by exposing the blot to α SUM1/2-specific antibodies or to α HIS antibodies that recognize the tagged *SUM3*) (Figures 3A and 3B).

High expressors of *SUM1*(Δ GG) or *SUM2*(Δ GG) showed a strong developmental phenotype in comparison to plants overexpressing *SUM1*(WT) or *SUM2*(WT) (Figures 3C to 3E; see Supplemental Table 1 and Supplemental Figure 4 online). The *SUM1*(WT) and *SUM2*(WT) overexpressors flowered early under SD conditions and had a compact rosette due to shortened petioles, while 35S-*SUM3*(WT) plants were only early flowering

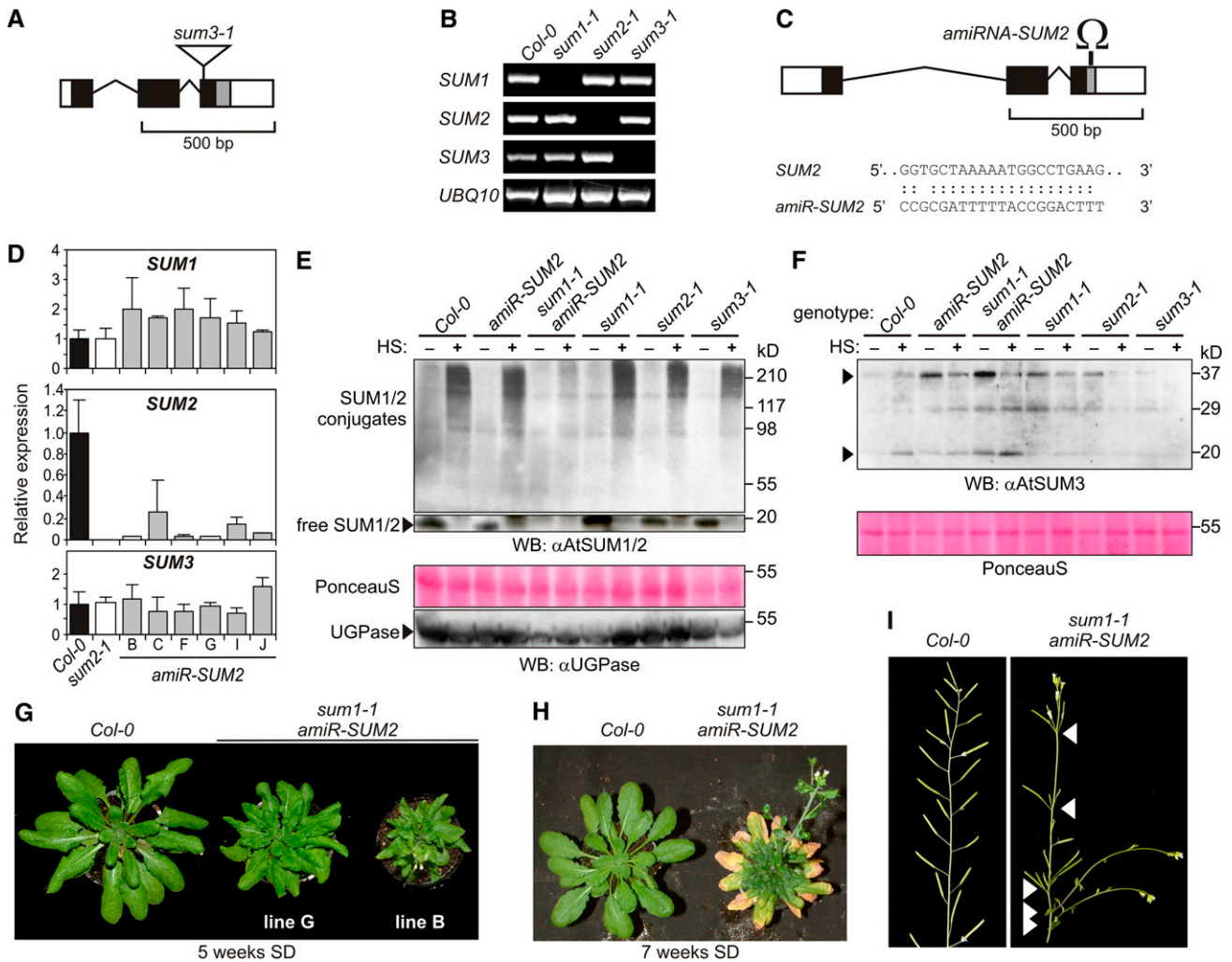


Figure 2. SUM1 and SUM2 Jointly Regulate Plant Development.

(A) To scale diagram of the *SUM3* gene and the location of the T-DNA insertion (arrowhead) that interrupts the reading frame at Met-78 in *sum3-1*. Exons and introns are represented by boxes and bent lines, respectively. White, black, and gray boxes reflect the 5'/3'-untranslated regions, the coding region of the mature SUM3 protein, and the C terminus removed during maturation, respectively.

(B) RT-PCR analysis confirmed the null alleles for the *sum1-1*, *sum2-1*, and *sum3-1* genotypes (wild-type *Col-0* was included as positive control, $n = 4$). Left, target gene amplified by PCR; top, genotype tested. PCR was performed for 30 cycles. *UBQ10* mRNA was amplified as a positive control for PCR amplification.

(C) To scale diagram of the *SUM2* gene with the *amiR-SUM2* target site indicated (Ω) in the C-terminal extension, which is removed during maturation. Schematic organization as in **(A)**. Bottom, the sequence of *amiR* and the target sequence in *SUM2*.

(D) Introduction of *amiR-SUM2* in *Arabidopsis* resulted in *SUM2* silencing without silencing of *SUM1* or *SUM3*, as shown using qRT-PCR. Wild-type (*Col-0*) and *sum2-1* were included as controls for *SUM2* expression. Depicted are the mean expression levels \pm SD. The biological samples ($n = 4$) were normalized using *TUB4* expression, and the y axis shows the relative expression levels of the *SUM* genes in the different lines compared with the level found in wild-type plants.

(E) Homozygous *sum1-1 amiR-SUM2* seedlings showed reduced levels of both free SUM1/2 and SUM1/2 conjugates in response to heat shock (HS). SUMO conjugation levels were detected in total protein extracts using antibody against SUM1/2 (α AtSUM1/2). PonceauS stain and the α UPGase immunoblot (WB: α UPGase) are shown as a control for equal protein loading. +, HS; -, no HS.

(F) The *sum1-1 amiR-SUM2* double knockdown showed increased accumulation of SUM3 protein (arrowheads). Other conditions the same as for **(E)**.

(G) to **(I)** *SUM1* and *SUM2* act redundantly in plant development, as independent *sum1 amiR-SUM2* lines showed strong dwarfism **(G)**, leaf crooking, occasional leaf fusion, shortened petioles, early leaf senescence combined with early flowering under SDs **(H)**, reduced apical dominance, partial sterility **(I)** (arrowheads pointing left), and disrupted inflorescence patterning leading to up to five developing siliques at single node positions (arrowheads pointing right).

Table 1. Flowering Analysis of the Single *sum* Mutants and the *sum1 amiR-SUM2* Double Knockdown Mutant

Plant Line	LD		SD		Post-Hoc ^c
	Mean \pm SD ^a	n ^b	Mean \pm SD	n	
Control (<i>Col-0</i>)	13.0 \pm 1.11	20	57.12 \pm 6.66	16	B
<i>sum1-1</i>	13.4 \pm 1.50	36	55.88 \pm 3.88	16	BC
<i>sum2-1</i>	13.4 \pm 2.12	22	56.3 \pm 3.4	14	BC
<i>sum3-1</i>	12.9 \pm 1.55	26	64.8 \pm 2.45	12	A
<i>sum1-1 amiR-SUM2</i> (line B)	8.3 \pm 1.55 ^d	18	37.4 \pm 2.85 ^d	17	E
<i>sum1-1 amiR-SUM2</i> (line G)	ND ^e		48.8 \pm 4.30 ^d	18	D
<i>amiR-SUM2</i> (line B)	12.8 \pm 2.12	20	59.7 \pm 2.84	15	B
<i>amiR-SUM2</i> (line G)	ND		61.6 \pm 4.25	21	AB

^aMean flowering time \pm SD (days).

^bNumber of plants examined.

^cBonferroni post-hoc testing with $P < 0.05$.

^dThe homozygous progeny from the cross between *sum1-1* and the *amiR-SUM2* flowered significantly early than the parental lines (Student's *t* test; $P < 0.05$).

^eND, not determined.

without exhibiting other visible growth phenotypes (Figure 3C). In addition, high expressors of SUM1(Δ GG) and SUM2(Δ GG) were partially sterile, exhibited disturbed internode patterning of the inflorescence stem, and showed pronounced senescence at the leaf periphery (Figures 3C to 3E). In fact, the growth phenotype of the high expressors of SUM1(Δ GG) and SUM2(Δ GG) closely resemble the phenotype of the *siz1* mutant, whereas intermediate expressors resemble a mild *sum1-1 amiR-SUM2* knockdown mutant (line G). Possibly, accumulation of SUM1(Δ GG) and SUM2(Δ GG) confers a dominant-negative effect on SIZ1 function. This effect was not found for SUM3(Δ GG) expressing lines.

In agreement with this, we noted that SUM3 protein levels never reached the high levels found for SUM1 or SUM2 when overexpressing the corresponding genes (Figure 3B, α HIS). We also observed that overexpression of SUM3(WT) or SUM3(Δ GG) did not alter SUM1/2 conjugation in any of the transgenic plants tested (Figure 3A, total protein extract; see Supplemental Figure 5 online). Likewise, we obtained a normal increase in SUM1/2 conjugation after heat shock in plants overexpressing SUM3, although the tagged SUM3 became conjugated to other proteins as a result of the heat shock (Figure 3B, compare lanes 2 and 8, middle panel). The reduced SUM3 protein levels correspond with reduced transcript levels of the *SUM3* transgene in comparison to the expression levels of *SUM1* and *SUM2* transgenes (see Supplemental Figure 6 online). This suggests that the absence of a clear phenotype for the SUM3(Δ GG)-overexpressing plants may at least in part be due to relatively low SUM3 protein levels.

Accumulation of SUMO1 or SUMO2 Paralogs Promotes SA-Dependent Defense Responses

The developmental defects of the *siz1* mutant are largely caused by constitutive activation of SA signaling upstream of PHYTOALEXIN DEFICIENT4 (PAD4) that results in increased disease resistance (Lee et al., 2007; Jin et al., 2008; Cheong et al., 2009;

Miura et al., 2010). Other phenotypes that are generally associated with constitutive SA signaling are spontaneous cell death, constitutive expression of pathogenesis-related (*PR*) genes, increased resistance to infection by *Pseudomonas syringae* pv *tomato* DC3000 (*Pst*DC3000), and reduced elicitor-dependent hypersensitive response (HR) (Rate and Greenberg, 2001; Devadas and Raina, 2002; Heil and Baldwin, 2002; Lorrain et al., 2003). We therefore examined whether overexpression of the SUMO variants resulted in constitutive activation of SA signaling. Overexpression of SUM1 or SUM2, but also of SUM3 (both WT and Δ GG) resulted in enhanced resistance to *Pst*DC3000 (maximum 100-fold reduced bacterial growth) and correspondingly reduced disease symptoms, such as chlorosis and water-soaked lesions (Figure 4).

We also examined whether overexpression of these SUMO variants reduced *avrRpm1*-mediated HR (the used ecotype Columbia-0 [*Col-0*] carries the cognate resistance gene *RPM1* required for recognition of *avrRpm1*) (Figure 5). High expressors of mature SUM1, SUM2, and SUM3 showed a strong reduction in HR as exemplified by the reduced ion leakage from the leaf discs upon infiltration of *Pst* expressing *avrRpm1* (Figure 5A). Similarly, high expressors of SUM1(Δ GG) and SUM2(Δ GG) also showed a strong reduction in ion leakage (Figure 5B). Interestingly, expression of SUM3(Δ GG) resulted in \sim 20% lower levels of ion leakage than control plants (*Col-0*). The reduction in ion leakage correlated in each case with a reduction in the number of leaves showing extensive trypan blue staining at 7 h after infiltration of *Pst* expressing *avrRpm1* (see Supplemental Figure 7 online), which confirms the reduced levels of cell death induction.

To further link these SUMO overexpression phenotypes to activation of SA-dependent defense responses, we determined the SA levels in these plants (Figure 5C). Several SUMO overexpression lines showed increased SA levels, similar to the *siz1-2* mutant. We noted a maximal 10-fold increase in SA-2-O- β -D-glucoside (SAG) levels in these lines. Concomitantly, expression of the SA marker gene *PR1* was >100 -fold increased in the 35S-SUM1 and 35S-SUM2 lines (both WT and Δ GG), while 35S-SUM3 lines showed up to 100 times increased expression of *PR1* (both WT and Δ GG) (Figure 5D). We could also show accumulation of the PR1 protein in these plants (Figure 5E). Enhanced exposure of the blot revealed accumulation of the PR1 protein also in the 35S-SUM3(Δ GG) lines (Figure 5F). Under SD conditions, accumulation of the PR1 protein was first observed in 4-week-old 35S-SUM2 (WT or Δ GG) plants (Figure 5G), whereas growth defects were already visible in 2- to 3-week-old plants. This suggested that the SUMO-dependent upregulation of *PR1* is in part age dependent, possibly involving progressive accumulation of free SUMO or SUMOylated proteins. The 35S-SUM1 (Δ GG)- and 35S-SUM2(Δ GG)-expressing plants also developed macroscopically visible lesions 6 to 8 weeks after germination under SD conditions (see Supplemental Figure 8A online). Trypan blue staining revealed that not only the Δ GG-expressing plants showed spontaneous cell death, but also the plants that overexpress mature SUMO (*SUM1*, *SUM2*, or *SUM3*) (see Supplemental Figure 8B online). Notably, overexpression of *SUM3* (Δ GG) did not result in spontaneous cell death. In conclusion, hyperaccumulation of each of the three SUMO paralogs resulted in activation of SA-dependent defense responses.

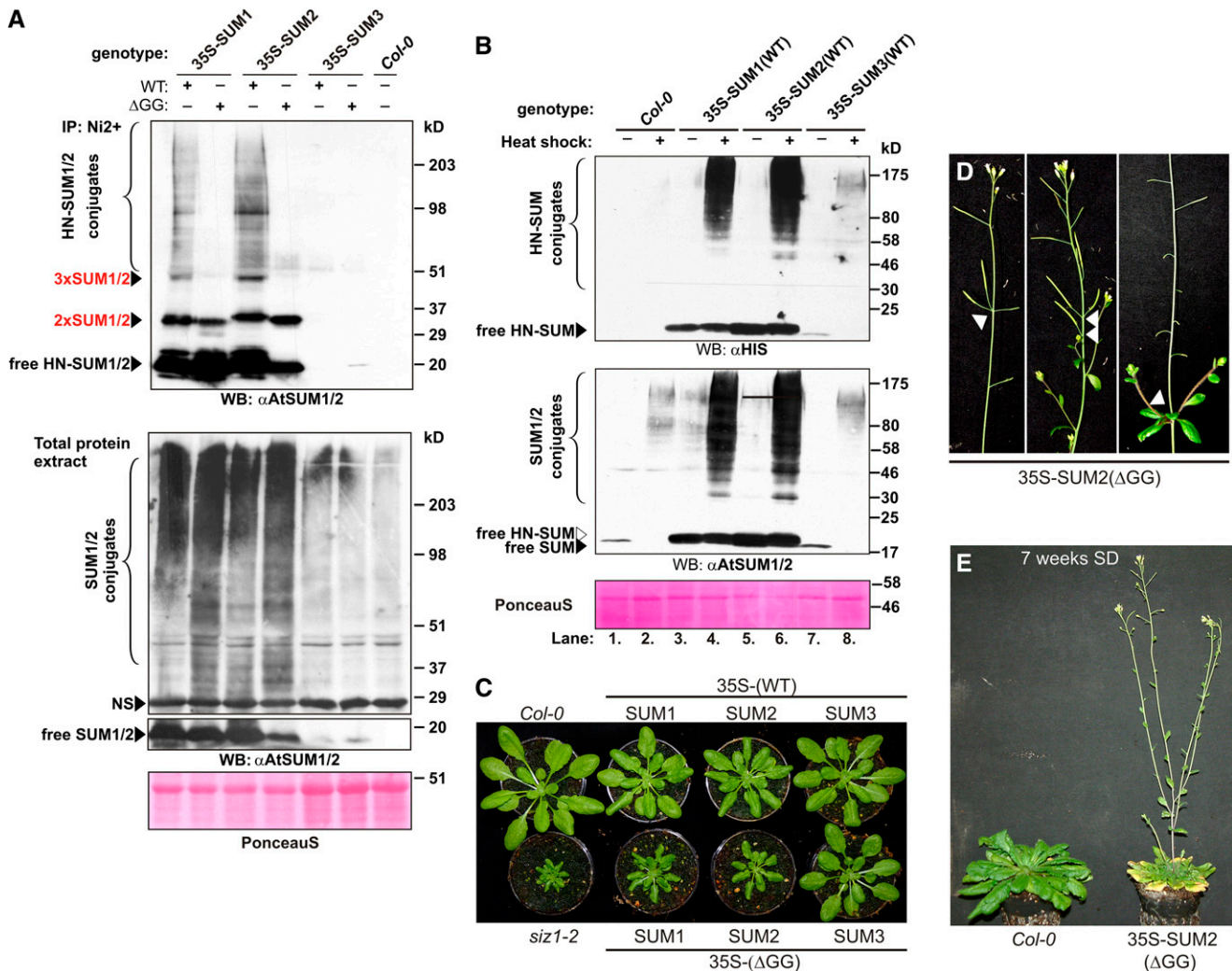


Figure 3. Overexpression of the Conjugation-Deficient Mutant SUM1(ΔGG) or SUM2(ΔGG) Resulted in Similar Growth Phenotypes as the *siz1* and *sum1 amiR-SUM2* Mutants.

(A) Overexpression of both mature (WT) and a conjugation-deficient (ΔGG) mutant of HN-tagged SUM1 and SUM2 resulted in increased SUM1/2 conjugation levels in 5-week-old plants. By contrast, overexpression of SUM3 (both WT and ΔGG) did not lead to increased conjugation of SUM1 or SUM2. SUM1(ΔGG) and SUM2(ΔGG) are not conjugated to target protein, but they are themselves SUMOylated by endogenous SUMO, resulting in a covalent SUMO dimer (2xSUM1/2). The wild type (*Col-0*) was included as control. Top panel (IP: Ni²⁺), pull-down of the HN-tagged protein fraction with Ni²⁺ resin; bottom panels, total protein extract (6 M GuCl and 20 mM NEM). Blots were probed with αAtSUM1/2 antibody. The nonspecific signal (NS) and PonceauS staining are shown as control for equal protein loading. 3xSUM1/2, protein complex containing three SUMO proteins.

(B) Seedlings overexpressing mature SUMO showed increased SUMOylation in response to heat shock compared with control plants (nontransgenic *Col-0*). HN-tagged SUM3(WT) is also conjugated to targets in response to heat shock (WB:αHIS, lane 8).

(C) Overexpression of SUM1(ΔGG) or SUM2(ΔGG) resulted in strong leaf curling, dwarfism, leaf crooking, and shortened petioles, similar to the *siz1* mutant. In comparison, overexpression of mature SUM1 and SUM2 (WT) protein caused mild dwarfism and reduced petiole length, while overexpression of SUM3 (WT and ΔGG) did not trigger any visible developmental defects. Plants were grown under SD conditions.

(D) Overexpression of SUM2(ΔGG) resulted in disturbed inflorescence patterning and partial sterility (arrowheads). Similar observations were made for SUM1(ΔGG).

(E) Overexpression of SUM2(ΔGG) resulted in early flowering and increased senescence. Plants were grown for 7 weeks under SD conditions.

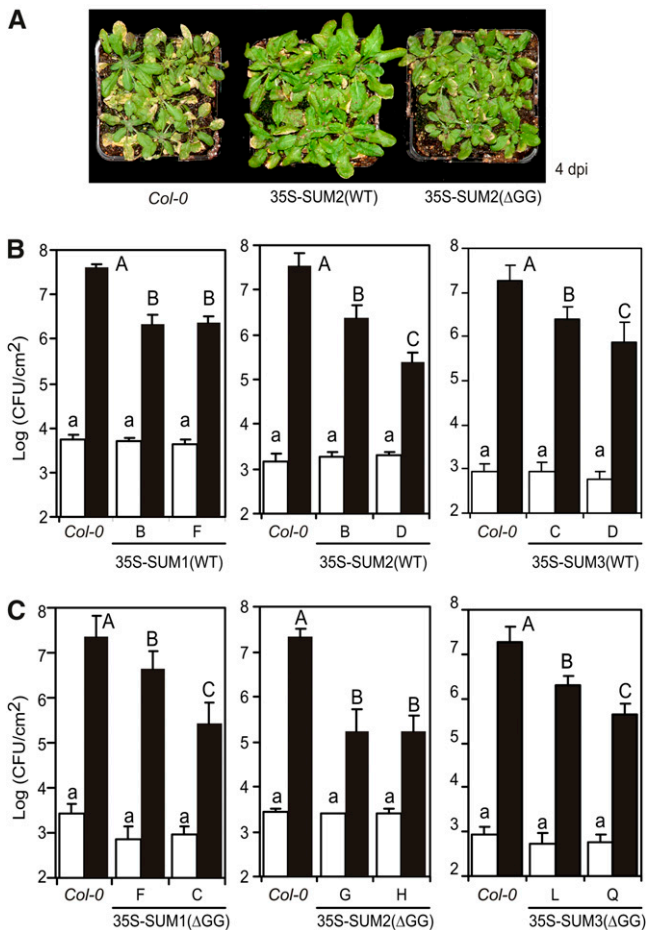


Figure 4. Overexpression of SUMO Variants in *Arabidopsis* Resulted in Increased Resistance to *PstDC3000*.

(A) *Arabidopsis* expressing 35S-SUM2 (WT or Δ GG) showed reduced disease symptoms (water-soaked lesions, chlorosis, and necrosis) in comparison to wild-type plants (*Col-0*). Photographs were taken 4 d postinoculation (dpi) with *PstDC3000*.

(B) Wild-type plants (*Col-0*) and two independent transgenic lines expressing relatively high levels of mature SUM1, SUM2, or SUM3 were inoculated with *PstDC3000*. Depicted are the mean log bacterial counts \pm SE (white bars, t = 0 dpi; black bars, t = 3 dpi). Different letters above the bars indicate significant differences in mean log bacterial count at $P = 0.05$ using an analysis of variance ($n = 8$ plants; lowercase a, t = 0 dpi; CAPS A/B/C, t = 3 dpi). The experiment was repeated three times with similar results.

(C) Similar as in **(B)**, except that plants tested expressed at relatively high levels a conjugation-deficient mutant (Δ GG) of the indicated SUMO paralog.

ICS1 Is Required for SUM2-Induced Disease Resistance Phenotypes and a Subset of the Developmental Phenotypes

To ascertain genetically that the growth and disease phenotypes caused by SUMO overexpression are SA dependent, the SUMO-overexpressing lines were crossed with the *sid2-1* (*SALICYLIC ACID INDUCTION DEFICIENT2*) mutant. The *sid2-1* line carries a null mutation in *ISOCHORISMATE SYNTHASE1* (*ICS1*)

(Wildermuth et al., 2001). *ICS1* is essential for SA synthesis following pathogen recognition, and the *sid2-1* allele allows normal plant growth (Wildermuth et al., 2001; Strawn et al., 2007; Garcion et al., 2008; Yaeno and Iba, 2008). The homozygous F2 progeny of the *sid2-1* 35S-SUM2(WT) and the *sid2-1* 35S-SUM2(Δ GG) crosses showed a partial reversion of the SUMO-dependent growth defects (i.e., leaf curling was lost but the plants remained dwarfed) (Figure 6A). In addition, the leaves did not fully elongate, resulting in shorter and more rounded leaves. We next examined the expression of several SA marker genes (*PR1*, *PR2*, *PR5*, and *PAD4*) in these crosses and in their parental lines (Figure 6B). Loss of a functional allele of *ICS1* reverted expression of these SA marker genes back to normal levels despite the overexpression of *SUM2* (WT or Δ GG). These genetic data confirm that overexpression of *SUM2* (WT or Δ GG) results in *ICS1*-dependent SA synthesis and subsequent expression of defense genes. Furthermore, not all 35S-SUM2-related developmental phenotypes can solely be attributed to SA accumulation.

SUM1 and SUM2 Jointly Suppress Activation of SA-Dependent Defense Responses

Considering that both the *sum1 amiR-SUM2* knockdown mutant and high expressors of SUM1(Δ GG) and SUM2(Δ GG) mimic the developmental phenotype of the *siz1* mutant, we examined whether *SUM1* and *SUM2* are involved in the regulation of SA-dependent innate immunity in noninfected plants. To this end, the different *sum* mutants were examined in *Pseudomonas* disease assays. None of the single *sum* knockout lines showed altered resistance to *PstDC3000* or exhibited reduced *avrRpm1*-mediated HR (Figures 7A and 7B). The *sum1-1 amiR-SUM2* knockdown, however, did show significantly increased resistance to *PstDC3000* (Figure 7C). In corroboration, we found that the *sum1-1 amiR-SUM2* lines showed fourfold to eightfold increased SAG levels in comparison to the parental lines, while the SA and SAG levels were not increased for the single *sum* knockout lines analyzed in parallel (Figure 7D). These *sum1-1 amiR-SUM2* double mutants showed 10-fold increased *PR1* expression in comparison to wild-type *Arabidopsis* (*Col-0*), whereas the corresponding single mutants did not show increased *PR1* expression (Figure 7E). In agreement with this, trypan blue staining revealed extensive microscopic cell death in 6- to 8-week-old rosette leaves (SD) of noninfected *sum1-1 amiR-SUM2* plants (Figure 7F). Cell death was not restricted to individual cells but occurred in larger clusters of mesophyll cells (lesions) and in the vasculature. This microscopic cell death was not observed in control plants (*Col-0*, *sum1-1*, and *sum2-1*). Hence, *SUM1* and *SUM2* are together essential to prevent increased SA accumulation and induction of SA-dependent gene expression in noninfected plants.

Expression of SUM3 but Not of SUM1 or SUM2 Is Highly Induced by SA Treatment

Considering that the *sum1 amiR-SUM2* plants showed both increased SA levels and increased SUM3 protein levels (Figures 7D and 2F, respectively), we examined whether SA accumulation causes induction of *SUM3*. Analysis of deposited transcriptome

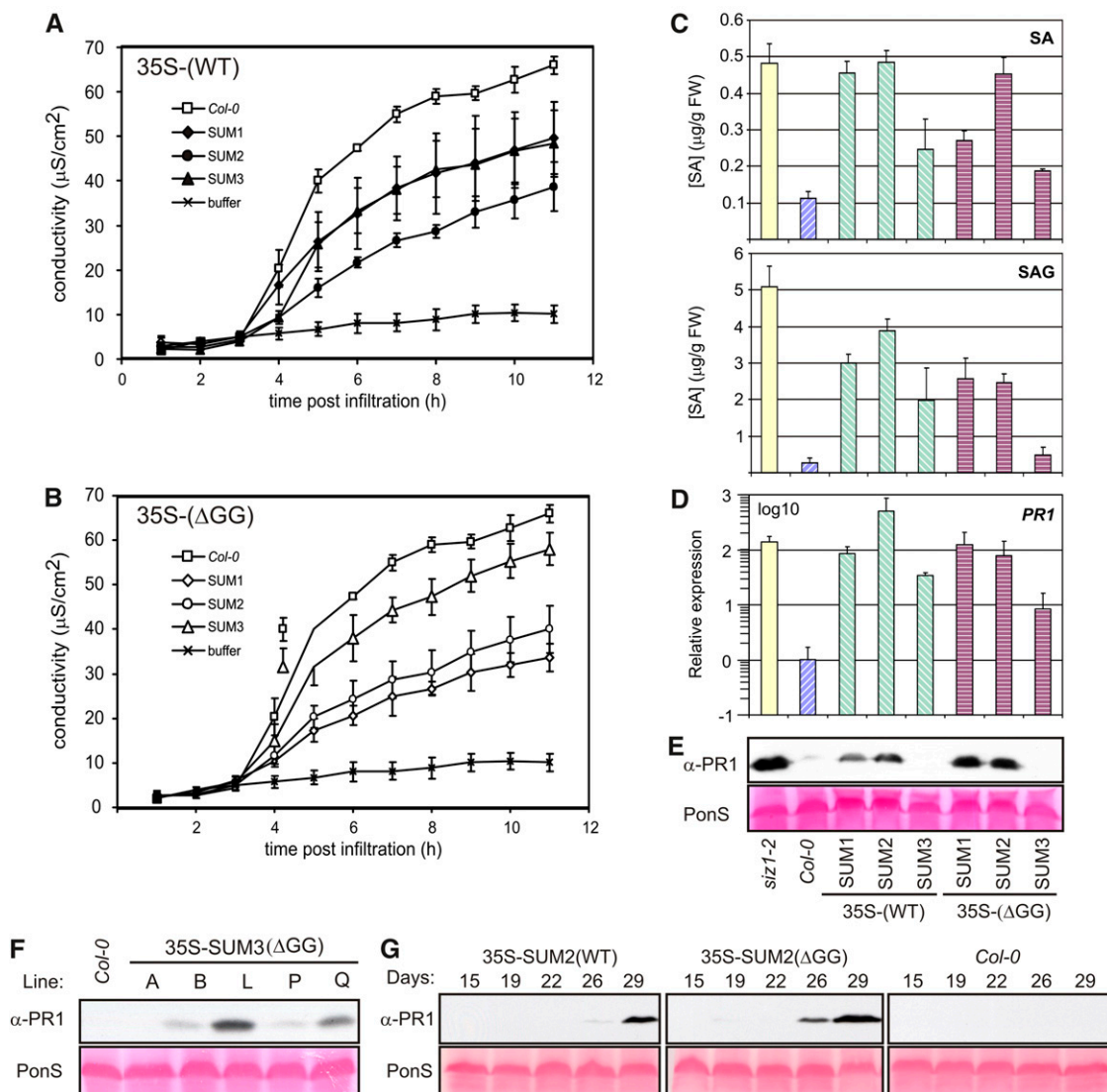


Figure 5. Overexpression of SUMO Variants in *Arabidopsis* Resulted in Reduced HR and Increased Accumulation of SA.

(A) Overexpression of mature SUMO paralogs (35S-WT) resulted in reduced HR (as indicated by reduced ion leakage compared with the control) upon inoculation with *Pst* expressing *avrRpm1*. Symbols represent the mean \pm SD conductivity measured per genotype. As negative control, buffer only (10 mM MgCl_2) was infiltrated in wild-type plants (*Col-0*).

(B) Similar as **(A)**, except that plants were tested that overexpress a conjugation-deficient SUMO mutant (35S- ΔGG).

(C) Overexpression of SUMO variants resulted in accumulation of free SA and SAG in 5-week-old SD-grown plants. As controls, the *siz1-2* mutant (yellow) and wild-type plants (*Col-0*; blue) were included (bars represent mean \pm SD; $n = 4$ samples per line).

(D) High expressors of 35S-SUM1 and -SUM2 (both WT and ΔGG) show increased expression of the SA marker gene *PR1*, similar to the *siz1* mutant, while 35S-SUM3 plants show intermediate expression of *PR1*. Expression levels were determined using qRT-PCR. RNA was extracted from 17-d-old LD-grown seedlings. The biological samples ($n = 4$) were normalized using TUB4 expression, and the mean expression of *PR1* in *Col-0* was set at 1. Experiment was repeated three times with similar results.

(E) Plants expressing high levels of SUM1 or SUM2 (both WT and ΔGG) showed accumulation of PR1 protein (αPR1 antibody) similar to the *siz1* mutant. Total protein extracts were prepared from 17-d-old seedlings grown under LD conditions. PonceauS (PonS) staining of the blot confirmed equal protein loading. At least two independent transgenic lines were examined per construct.

(F) Similar as in **(E)**, except that enhanced exposure of the blot revealed that transgenic lines overexpressing 35S-SUM3(ΔGG) also showed increased PR1 protein accumulation. PR1 protein levels in these lines were lower than those observed for 35S-SUM1 and 35S-SUM2 (both WT and ΔGG), as shown in Figure 3E.

(G) Similar as in **(E)**, except that total protein extracts were prepared from plants grown under SD conditions. Top: genotype tested (top). Accumulation of the PR1 protein is age dependent in plants that overexpress SUM2 variants.

[See online article for color version of this figure.]

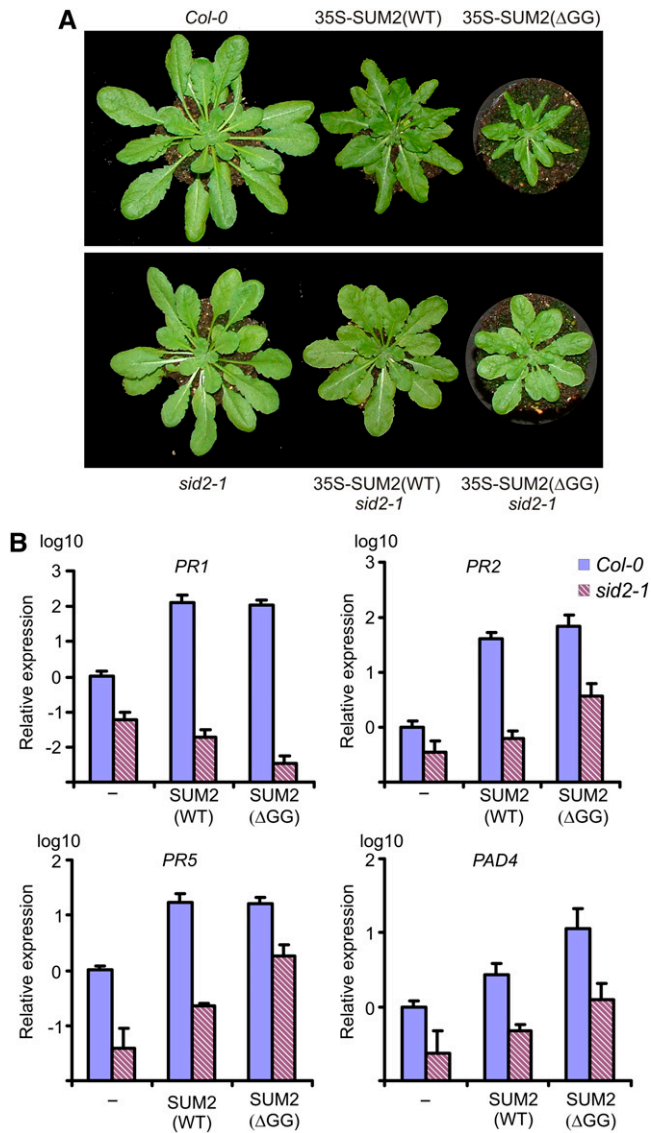


Figure 6. The Developmental Phenotype Caused by Overexpression of SUM2 Variants Is Largely *ICS1* (*SID2*) Dependent.

(A) Developmental phenotype of 35S-SUM2 (both WT and ΔGG) plants was largely *ICS1* dependent. The *sid2-1* allele of *ICS1* is in the *Col-0* background.

(B) Induction of the SA-marker genes (*PR1*, *PR2*, *PR5*, and *PAD4*) following overexpression of mature SUM2 (WT or ΔGG) is *ICS1* dependent. Relative expression levels were determined for the indicated genes using qRT-PCR in 4-week-old plants grown under SDs. Individual biological samples ($n = 4$ with two technical replicates per plate) were normalized against TUB4 expression, and the mean expression in the control (*Col-0*) was set at 1 ($\log_{10} = 0$). Error bars represent sd.

[See online article for color version of this figure.]

data indicated that expression of *SUM3* is indeed induced by the SA analog benzothiadiazole (Thibaud-Nissen et al., 2006; Wang et al., 2006). Moreover, *SUM3* expression is also increased in the *siz1* mutant (Catala et al., 2007). These same microarray data sets did not indicate altered expression of the *SUM1* or *SUM2*

genes in either the *siz1* mutant or after SA application. We therefore examined the *SUM3* expression profile after SA treatment (Figure 8A). Using quantitative RT-PCR (qRT-PCR), we found that SA treatment strongly induces *SUM3* expression, but only transiently, peaking 3 h after SA application. At this time point, *SUM3* expression was 80-fold increased compared with mock-treated plants. The SA-dependent induction of *SUM3* appeared to be paralog specific, as expression of *SUM2* was hardly induced by either mock or SA treatment, and expression *SUM1* was only modestly increased by SA treatment. An analysis using the *SUM3* promoter-GUS lines confirmed the SA sensitivity of the *SUM3* promoter (Figures 8B and 8C). Moreover, expression of *SUM3* was no longer restricted to the leaf vasculature and hydathodes, as GUS staining could be detected in mesophyll cells after SA treatment. In parallel, we confirmed that GUS staining was not increased in the *SUM1* and *SUM2* promoter-GUS reporter lines after SA treatment. Subsequently, we tested whether *SUM3* can be induced by the Flg22 peptide, a 22-residue peptide that acts as general elicitor of plant defense responses and is derived from bacterial flagellin (Zipfel et al., 2004). Infiltration with 10 μ M Flg22 peptide resulted in a transient induction of *SUM3* within 6 h, while infiltration with the negative control (Flg22^{atum} peptide) triggered a modest induction of *SUM3* at 9 h (Figure 8D). Upregulation of *SUM3* required *ICS1*, confirming strict regulation of the expression of *SUM3* downstream of SA after perception of the Flg22 peptide by the FLS2 receptor. By contrast, *SUM1* and *SUM2* expression was not substantially altered by infiltration with the Flg22 peptide. As an additional control, we confirmed that *PR1* was only highly induced in wild-type plants (*Col-0*) and not in *sid2-1* plants after infiltration with the Flg22 peptide (Figure 8D). These data are supported by microarray data showing that *SUM3* is induced after infection by *Pseudomonas* (6 to 16 h after infection by *Pst* DC3000 and *P. s. pv maculicola* strain ES4326) (Journot-Catalino et al., 2006; Thilmony et al., 2006; Underwood et al., 2007; Winter et al., 2007). We also examined SUM3 protein levels after SA treatment (see Supplemental Figure 9 online). We found that the SUM3 conjugation profiles did not change in 35S-SUM3(WT) plants after SA treatment or treatment with the proteasome inhibitor MG132. However, we noted that free HN-tagged SUM3 became subject to an apparent posttranslational modification (hnSUM3*) as a result of the SA treatment. This implies a functional link between *SUM3* expression, SUM3 protein accumulation, and SA signaling. We conclude that induction of *SUM3* appears to be part of the endogenous defense signaling cascade in *Arabidopsis* and, since induction of *SUM3* preceded expression of *PR1*, SUM3 conjugation might regulate (part of) the SA-dependent defense responses.

DISCUSSION

SUM1 and *SUM2* Regulate Plant Development and Jointly Suppress Activation of SA-Dependent Signaling

Here, we establish distinct biological functions for the *Arabidopsis* SUMO paralogs in development and innate immunity. The *sum1 amiR-SUM2* knockdown mutant showed that *SUM1* and

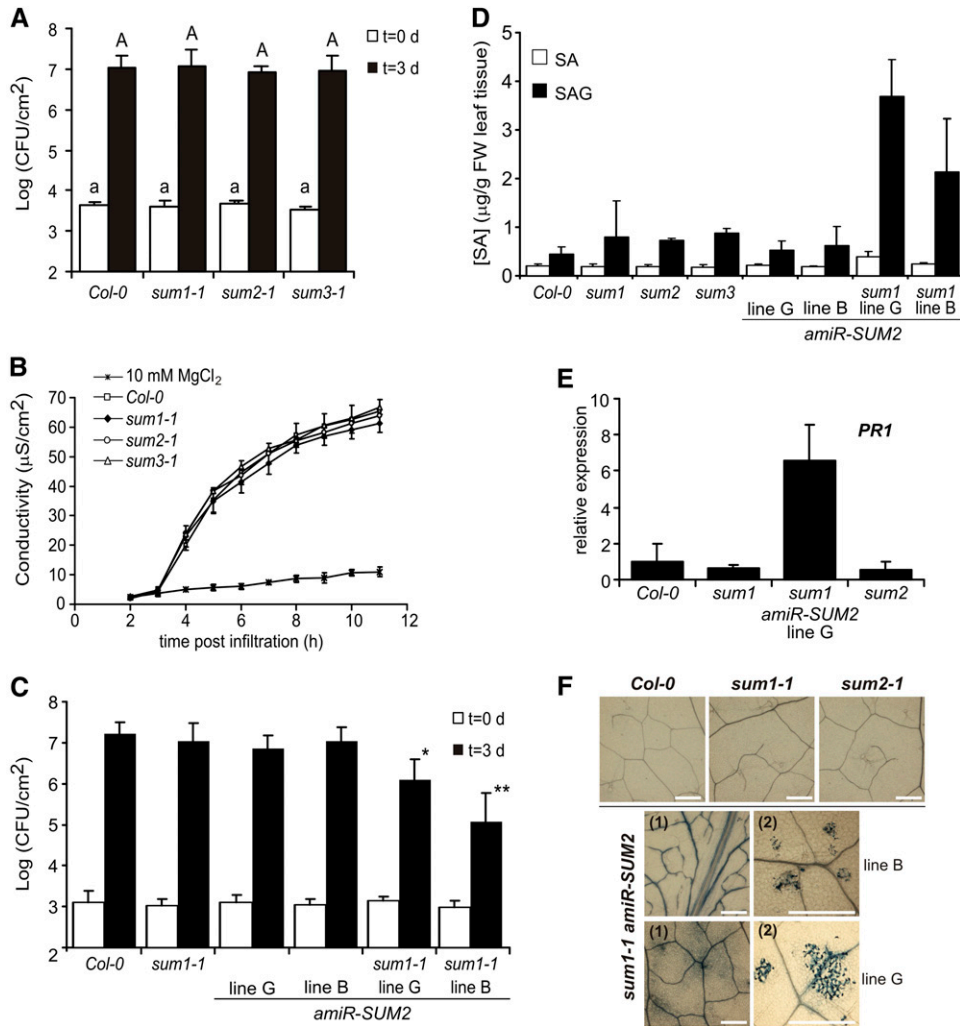


Figure 7. SUM1 and SUM2 Together Are Essential to Prevent Constitutive Activation of SA-Dependent Plant Defense Responses.

(A) *SUM* null alleles (*sum1-1*, *sum2-1*, and *sum3-1*) did not show significantly different resistance to *PstDC3000* than the control (wild-type *Col-0*), as determined by analysis of variance of the mean log bacterial count at *t* = 0 d (group a) or *t* = 3 d (group A). Depicted are mean log bacterial counts ± SE (*n* = 8 samples). Data are from one representative experiment (*n* = 3).

(B) Loss of a single SUMO paralog did not impair ion leakage (HR induction) triggered by *Pst* expressing *avrRpm1*. Means ± SD were determined using four leaf discs per genotype. Symbols represent the genotypes indicated. As control, we infiltrated leaf discs with buffer only (10 mM MgCl₂). Data are from one representative experiment (*n* = 3).

(C) The *sum1-1 amiR-SUM2* double mutant shows enhanced resistance to *PstDC3000*. Depicted is mean log bacterial growth ± SE (*n* = 8) for two independent crosses of *sum1-1 amiR-SUM2* (lines B and G) and the parental lines. The asterisk above the bars indicates significant differences in mean log bacterial count at **P* = 0.05 and ***P* = 0.01 (pair-wise Student's *t* test with the parents). The assay was repeated three times with similar results.

(D) The *sum1-1 amiR-SUM2* double mutant showed increased accumulation of free SA and SAG in comparison to the parental lines and wild-type plants (*Col-0*). Bars represent means ± SD (*n* = 4). Five-week-old SD-grown plants were sampled. The assay was repeated three times with similar results. FW, fresh weight.

(E) The *sum1-1 amiR-SUM2* double mutant showed at least 10-fold increased *PR1* expression levels compared with control plants. RNA was extracted from 17-d-old seedlings grown under LD conditions. Individual biological samples were normalized against TUB4 expression, and the mean expression in the wild-type plants (*Col-0*) was set to 1.

(F) The *sum1-1 amiR-SUM2* double mutant developed spontaneous cell death in the vasculature (1) and individual cells and cells clusters (2). Cell death was visualized using lactophenol trypan blue staining. Wild-type (*Col-0*), *sum1-1*, and *sum2-1* plants did not show cell death at the same stage of plant development. Bar = 500 µM.

[See online article for color version of this figure.]

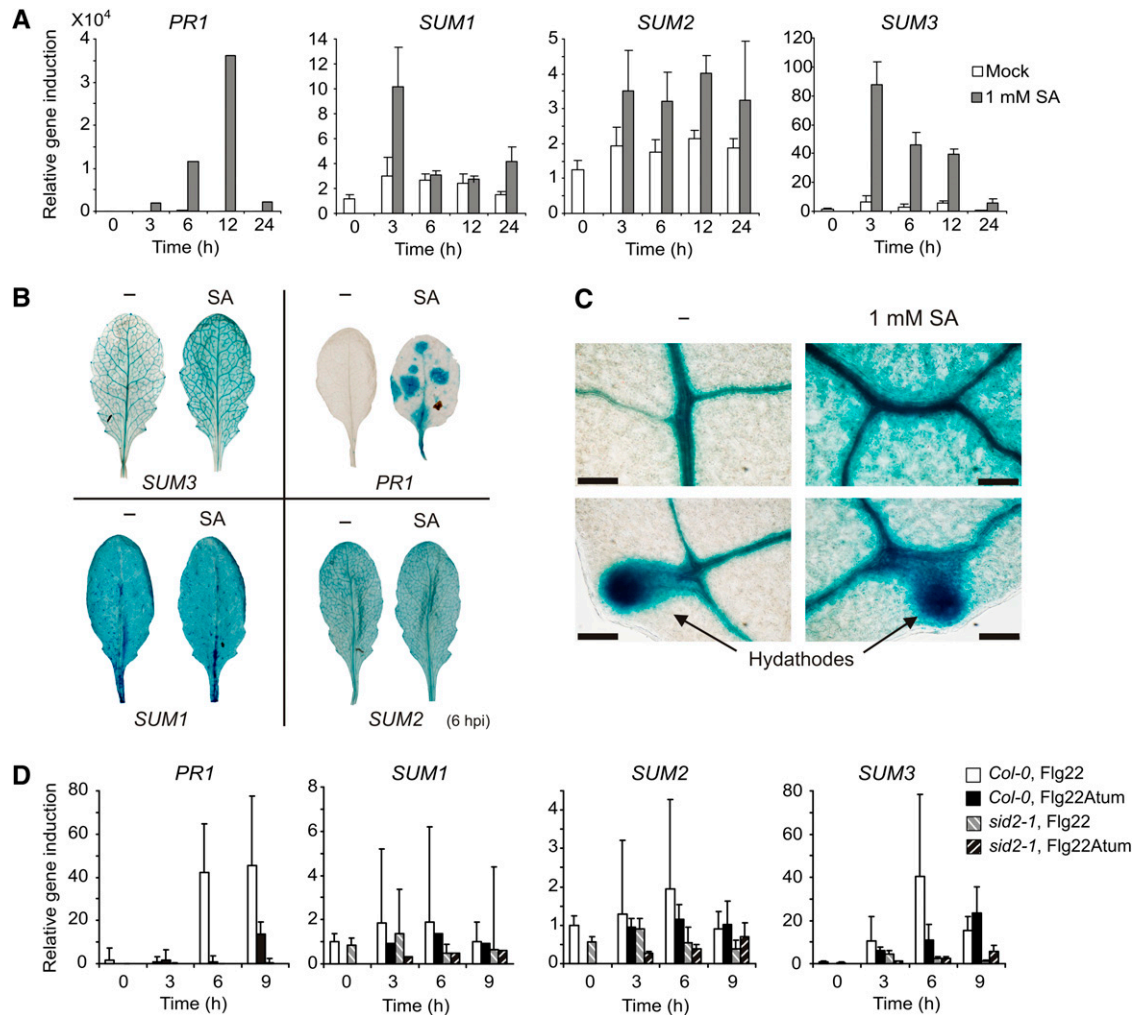


Figure 8. *SUM3* Is Rapidly and Transiently Induced by Flg22 Treatment in an SA-Dependent Manner.

(A) Expression levels of *SUM1*, *SUM2*, *SUM3*, and *PR1* were determined with qPCR over a time course of 24 h after subjecting 4-week-old plants to 1 mM SA (gray bars) or mock treatment (white bars). Both *SUM3* (>80-fold) and *SUM1* (3- to 5-fold) showed a transient increase in expression in response to SA. Biological samples were normalized using TUB4 expression levels, and the average expression levels of the four genes was scaled to 1 for t = 0. Four biological samples were taken per time point, and the error bars represent SD. Data are from one representative experiment (n = 3).

(B) Localization of GUS reporter activity in *Arabidopsis* expressing the GUS reporter gene under the control of the *SUM1*, *SUM2*, or *SUM3* promoters 6 h after treatment with 1 mM SA or mock treatment (-). Only the *SUM3* promoter is SA sensitive based on GUS staining intensities. Similar observations were made for two other *ProSUM3-GUS* lines. The *ProPR1-GUS* line (*PR1*) is shown as a positive control for SA-dependent gene induction. hpi, hours post infection.

(C) Magnification of the *Arabidopsis ProSUM3-GUS* leaves 6 h after treatment with SA or mock treatment (-) revealed GUS staining in leaf mesophyll cells in response to SA treatment. Bar = 100 μM.

(D) Expression of *SUM1*, *SUM2*, and *SUM3* and the SA marker gene *PR1* at various time points after infiltration with 10 μM Flg22 (white and gray hatched bars) or Flg22^{Atum} peptide (black [hatched] bars) in 4-week-old plants. Both wild-type (*Col-0*) and *sid2-1* plant were infiltrated, and samples were taken at the indicated times. The average expression levels ± SD of the tested genes were scaled to 1 for t = 0 h. Data are from one representative experiment (n = 3).

SUM2 act as basal regulators of normal plant development, prevent activation of defense responses in noninfected plants (Figure 9A), and prevent premature flowering. These functions of *SUM1* and *SUM2* are consistent with the constitutive expression of the corresponding genes. Our expression studies suggested a more generic role for *SUM1* and a more specialized role for

SUM2 in the leaf vasculature. Nevertheless, the individual *sum1* or *sum2* null mutants do not have obvious growth abnormalities (Saracco et al., 2007). Expression of *SUM3* is generally very low and restricted to a few cell types, but its expression is highly, transiently, and widely induced by SA. Thus, expression of these three *SUM* genes is differentially regulated in both time and space.

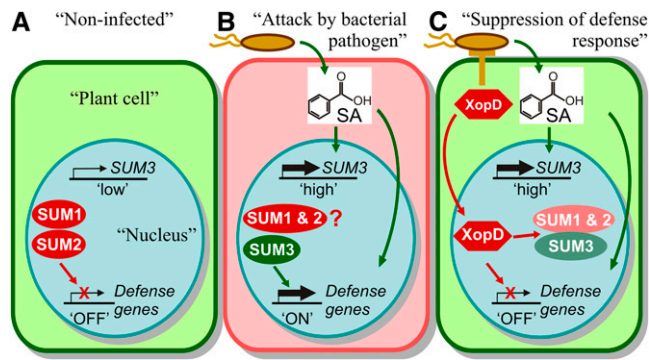


Figure 9. Model for the Regulation of SA-Dependent Defense Responses by the *Arabidopsis* SUMO Paralogs SUM1, SUM2, and SUM3.

(A) In noninfected plants, the *SUM1* and *SUM2* genes are constitutively expressed and the gene products inhibit (in a SIZ1-dependent manner) expression of SA-responsive defense genes, while expression levels of the *SUM3* gene are low.

(B) Recognition of a bacterial infection (e.g., by Flg22 perception) results in SA accumulation, which transiently induces *SUM3* expression and induction of SA-responsive defense genes. Accumulation of SUM3 protein promotes plant defense.

(C) The bacterial effector XopD from *Xanthomonas* is injected in host cell via the type three secretion system and inhibits plant defense gene expression via a transcriptional repressor domain. In addition, XopD contains a SUMO protease domain with SUMO protease activity toward SUM1- and SUM2-modified but also SUM3-modified proteins. Both biochemical activities (transcriptional repression and SUMO protease activity) result in enhanced virulence of bacteria expressing XopD.

SUM1 and SUM2 Exert Their Functions in Development and Defense via the SUMO E3 Ligase SIZ1

The functions of *SUM1* and *SUM2* in development and SA signaling mimic that of the gene encoding the SUMO E3 ligase SIZ1. *SIZ1* suppresses SA-dependent defense responses upstream of *PAD4* in noninfected plants (Lee et al., 2007). The *siz1* mutant and the *sum1 amiR-SUM2* knockdown mutants show similar growth defects. Furthermore, the *siz1* mutant has largely lost mass conjugation of SUM1 and SUM2 proteins in response to heat shock, linking SIZ1 protein function to SUM1 and SUM2 conjugation (Cheong et al., 2009). We found that hyperaccumulation of the conjugation-deficient mutants SUM1(Δ GG) and SUM2(Δ GG), but not SUM3(Δ GG), results in a dose-dependent growth phenotype, again closely resembling the *siz1* mutant, and, similar to *siz1* (Miura et al., 2010), these growth defects were largely SA dependent (Figure 6). Together, these data suggest that both SUM1(Δ GG) and SUM2(Δ GG) can inhibit SIZ1 function in vivo. Such an inhibition of SIZ1 function by binding of non-functional SUMO variants is conceivable, as the in planta SIZ1 protein levels are low and SUM1(Δ GG) can interact with SIZ1 in the yeast split-ubiquitin system (Cheong et al., 2009). This SUM1-SIZ1 protein interaction does not depend on the major protein domains of SIZ1 (SAP, PHD, SP-RING, or PINIT domains), but likely involves binding of SUMO to the SIM of SIZ1 (Garcia-Dominguez et al., 2008; Cheong et al., 2009). Complementation studies of the *siz1* mutant revealed that point muta-

tions in the SIM motif could not fully complement the SA-dependent phenotypes, and a functional SUMO E3 ligase domain (SP-RING) was essential to complement these phenotypes (Cheong et al., 2009). Based on these observations, we hypothesize that SIZ1 promotes conjugation of SUM1 or SUM2 to unknown negative regulator(s) of SA signaling that need(s) to be SUMOylated in noninfected plants (Figure 9A). Apparently, SUMOylation of this regulator depends on the SIM in SIZ1. SIZ1 is the plant prototype of yeast SIZ1 and the mammalian PIAS proteins, which regulate gene expression via chromatin remodeling (Miura et al., 2007a; Garcia-Dominguez et al., 2008; Rytinki et al., 2009). Also in yeast and mammals, the function of the SIZ1 homologs depends on their capability to noncovalently interact with SUMO via their SIM (Reindle et al., 2006; Rytinki et al., 2009). Based on this analogy, we have proposed before that SUMOylation of chromatin modifying enzymes and/or transcription factors inhibits transcription of a regulator(s) of the SA signaling pathway (van den Burg and Takken, 2009). Further studies are needed to elucidate the exact role of these SUMO paralogs and SIZ1 in the regulation of SA-sensitive gene expression.

Is Tight Regulation of SUM1 and SUM2 Expression Important for Proper Plant Development and Repression of Innate Immunity?

Proper plant development and repression of innate immunity in noninfected plants likely require tight regulation of *SUM1* and *SUM2* genes in planta, as hyperaccumulation of both WT and Δ GG resulted in activation of SA-dependent innate immunity rather than suppression. In addition, we and others have shown that overexpression of SUM1 and SUM2 variants results in enhanced SUM1/2 conjugation in plants (this study; Lois et al., 2003; Murtas et al., 2003). The other studies did not report SUM1- or SUM2-related growth defects related to overexpression (Lois et al., 2003; Murtas et al., 2003). However, when we reanalyzed plants that overexpress His-tagged SUM1 (Lois et al., 2003), we found increased expression of the SA marker gene *PR1* (see Supplemental Figures 10A to 10C online), showing that overexpression of SUM1 induces host defenses. We cannot exclude that some of the mild growth defects observed in our study can be attributed to the tag used, as N-terminal labeling of SUMO with relatively large peptide tags can interfere with SUMO protein function (Wohlschlegel et al., 2004; Budhiraja et al., 2009). However, our HN-tagged SUMO proteins were successfully used as substrates for SUMOylation in planta (Figure 3), and increased expression resulted in increased SUMOylation levels, demonstrating their functionality. Therefore, we propose that the SIZ-related phenotypes induced by overexpression of either the mature form or the Δ GG mutant are likely SIM dependent without inhibiting SIM-independent SUMO conjugation by SCE1 (as evidenced by the increased SUMOylation levels). This implies that SIZ1 function in SA signaling can be inhibited in planta by an excess of free SUMO. This requires that the levels of free SUM1 and SUM2 in wild-type plants be relatively low, which is indeed the case (Saracco et al., 2007). Alternatively, the increase in SUM1/2 conjugation levels due to overexpression of SUM1 and 2 variants could be caused by product inhibition of

SUM1/2-specific SUMO proteases (like ESD4, OTS1, and OTS2). Product inhibition has been reported as a result of overexpression of WT and Δ GG mutants of mammalian SUMO paralogs (Shen et al., 2006; Ihara et al., 2007; Mukhopadhyay and Dasso, 2007).

Whereas SUM3(Δ GG) overexpression did not increase SUM3 conjugation in plants, SUM3(WT) overexpression did induce a modest increase. In both cases, the overall SUM1/2 conjugation levels remained unaffected, which can be explained in two ways. First, SUM3 did not accumulate to the same high protein levels as the SUM1 and SUM2 proteins; hence, SUM3 might not reach SUMO protease inhibitory concentrations. Second, none of the known SUM1- and SUM2-specific SUMO proteases has isopeptidase activity toward SUM3 conjugates (Chosed et al., 2006; Colby et al., 2006). This means that SUM3 is unlikely to inhibit these SUM1- and SUM2-specific proteases. In summary, the increased SUMOylation levels upon SUM1 and SUM2 overexpression could be due to product inhibition of SUMO proteases that are not inhibited by the relatively low levels of SUM3. Additional studies should reveal which SUMO proteases are important for SA-dependent signaling.

SA-Dependent SUM3 Expression Promotes Plant Defense Responses and Flowering

Interestingly, activation of plant defense responses lifts the SUM1- and SUM2-dependent inhibition of SA signaling via an unknown mechanism and allows accumulation of SA, which subsequently triggers SUM3 expression and SUM3 protein accumulation (Figure 9B). Free SUM3 protein appears to be subject to an unknown posttranslational modification as a result of SA signaling. It has already been shown that mammalian SUMO1 is subject to phosphorylation in the N-terminal tail, but the conditions that induce this modification are unknown (Matic et al., 2008). Overall, we find that SUM3 appears to act downstream of SA synthesis, but upstream of plant defense responses, since overexpression of SUM3 resulted in PR1 expression and increased resistance.

The autonomous pathway promotes flowering during the juvenile-to-adult transition by downregulating FLOWERING LOCUS C (FLC) expression (Baurle and Dean, 2006). Repression of the autonomous flowering pathway appears to involve SIZ1-dependent SUMOylation because SIZ1 is required for full FLC expression (Jin et al., 2008). In agreement, we find that SUM1 and SUM2, like SIZ1, suppress flowering under both SD and LD conditions. In part, SIZ1 inhibits flowering by promoting SUMOylation of FLOWERING LOCUS D, a transcriptional repressor of FLC. More importantly, SIZ1-dependent inhibition of flowering appears to involve suppression of SA accumulation in adult plants (Jin et al., 2008). In wild-type adult plants, SA accumulation stimulates the autonomous pathway by repressing FLC expression via an unknown mechanism (Martinez et al., 2004). This age-dependent accumulation of SA might also allow expression of SUM3. In agreement, SUM3 was not expressed in juvenile leaves, but SUM3 became increasingly expressed in the leaf vasculature of adult plants (6- to 8-week-old plants). Moreover, the sum3 mutant displayed delayed flowering, while SUM3 overexpression promoted flowering under SDs. This signifies that the function of SUM3 differs from that of SUM1 and SUM2 in

flowering and SA-dependent responses. However, the sum3 mutant did not exhibit increased susceptibility to *PstDC3000*, which indicates that the function of SUM3 in plant defense could be redundant.

SUM3 is normally not extensively conjugated to other proteins, and its conjugation does not increase after a heat shock (Kurepa et al., 2003). However, transient overexpression of SUM3 does increase overall SUM3 conjugation (Budhiraja et al., 2009). This implies that SA-dependent accumulation of SUM3 will result in a transient increase in SUM3 conjugation. It remains to be determined whether this SA-dependent induction of SUM3 affects a common set of SUMO targets or concerns SUM3-specific targets. In support of the latter, a proteomics screen established that the set of SUM3 conjugates only partially overlapped with SUM1 and SUM5 conjugates identified (Budhiraja et al., 2009).

A prediction from the proposed function of SUM3 in pathogen defense is that inhibition of SUM3 conjugation should result in enhanced susceptibility to plant pathogens. Indeed, the effector protein XopD (*Xanthomonas* outer protein D) from the tomato (*Solanum lycopersicum*) pathogen *Xanthomonas campestris* pv *vesicatoria* is known to act as a SUMO isopeptidase in planta, and this activity enhances virulence of this pathogen on tomato (Hotson et al., 2003; Kim et al., 2008). Interestingly, XopD appears to have SUMO isopeptidase activity not only toward SUM1 and SUM2 conjugates, but also toward SUM3 conjugates (Colby et al., 2006). It is tempting to speculate that XopD isopeptidase activity might be targeted in vivo toward SUM3 conjugates to dampen host innate immune responses (Figure 9C). Identification of these SUM3 targets and investigation of their role in plant defense can put this model to the test. In conclusion, SUM1 and SUM2 together inhibit activation of SA-dependent responses in noninfected plants, whereas SUM3 appears to potentiate these responses following recognition of pathogen infection.

METHODS

Plant Material

Plants were grown at 21°C with 70% humidity under 40-W cool white fluorescent lights (100 to 150 mol m⁻² s⁻¹ photon flux density) under LDs (16 h light and 8 h dark) or SDs (9 h light and 15 h dark). The sum3-1 TDNA transposon insertion line (accession codes SM_3_2707/SM_3_21645) (Tissier et al., 1999) was obtained via the Nottingham Arabidopsis Stock Centre. *Arabidopsis thaliana* ProPR1-GUS (Shapiro and Zhang, 2001) and the *Arabidopsis* mutants *sid2-1* (Wildermuth et al., 2001), *sum1-1*, *sum2-1* (Saracco et al., 2007), and *siz1-2* (Miura et al., 2005) are described elsewhere. All plant transformations were performed in *Arabidopsis* ecotype Col-0. Progeny seeds were selected on 1× Murashige and Skoog (Duchefa) with 1% sucrose and 0.8% agar containing 50 mg/L kanamycin or 10 mg/L phosphinothricin.

GUS Assay

GUS assays (Jefferson et al., 1987) were performed on nonfixed *Arabidopsis* tissue at different developmental stages. GUS localization was observed after staining with 0.5 mg/mL 5-bromo-4-chloro-3-indolyl- β -D-glucuronide. The observed expression patterns were based on at least four independent transgenic lines showing similar GUS staining patterns.

Measurement of SA Levels (Free and 2-O- β -D-Glucoside)

SA extraction was performed according to Verberne et al. (2002). Leaf material (200 to 300 mg) was homogenized (FastPrep, 2 \times 45s) in 90% methanol spiked with 200 ng SA-d4 (internal control for extraction efficiency), followed by 100% methanol extraction. The organic phases were combined, vacuum-dried (Speed-Vac), and resuspended in warm water. The samples were buffered to a pH of 4.5 in 0.1 M NaAcetate and split in half. To one sample, almond β -glucosidase (Sigma-Aldrich) was added to hydrolyze SAG to SA. Both samples were incubated at 37°C overnight, followed by two extractions with an organic phase (50:50:1 mixture of cyclohexane/ethyl acetate/isopropanol). The organic phases were combined, dried (Speed-Vac without heating), and redissolved in 70% methanol for liquid chromatography–mass spectrometry analysis. Liquid chromatography–mass spectrometry settings were as described (Diezel et al., 2009). The ratios of ion intensities were determined for m/z 137 (daughter ion m/z 93) and m/z 141 (daughter ion m/z 97) for SA and SA-d4, respectively.

Constructs

For the promoter-GUS reporter assays, an \sim 2-kb DNA fragment upstream (5') of the start codon was cloned and fused to the GUS reporter in pEpiGreenB (pGreenII 0229 derivative; <http://www.pgreen.ac.uk/>). The resulting promoter-GUS fusions were used for stable transformation of *Arabidopsis*.

The protein tag consisted of the HIS tag and the streptavidin binding peptide NANO15-tag (HN-tag) fused to the free N terminus (Lamla and Erdmann, 2004). Expression of the chimaeras was driven by the 35S promoter. The tandem-affinity tag was created by overlap PCR amplification and directly cloned in the *Clal*-*Bam*HI sites of pEpiGreenB. The DNA fragments corresponding to mature SUMO protein (i.e., SUM1 [2 to 93 amino acids], SUM2 [2 to 92 amino acids], and SUM3 [2 to 93 amino acids]) or SUMO (Δ GG) were PCR amplified using cDNA from *Arabidopsis* Col-0 as template and cloned in the *Bam*HI and *Xba*I sites of pEpiGreenB. This created a 5' \rightarrow 3' Pro35S-His/Nano15-SUMOx-NOS terminator fusion construct.

The *amiR-SUM2* was engineered and PCR amplified from the miR319a backbone (pRS300) according to the instructions of Web MicroRNA Designer (Schwab et al., 2006). The resulting PCR fragment was subcloned in the *Clal*-*Xba*I of pEpiGreenK (pGreenII0029 derivative), creating a *Pro35S-amiR-SUM2-NOS* terminator fusion construct. All final fragments were sequenced. Transgenic plants were generated by floral dipping using *Agrobacterium tumefaciens* strain GV3101 (Clough and Bent, 1998).

Pseudomonas Disease Assays

Fresh cultures of *Pst*DC3000 strains were streaked from glycerol stocks onto selective King's B plates containing kanamycin (25 mg/mL) and rifampicin (25 mg/mL) and grown at 28°C. For plant inoculations, bacteria were grown overnight on King's B plates. Bacterial cells were scraped from the plates and suspended in 10 mM MgCl₂-100 mM sucrose to a final OD₆₀₀ of 0.1. Dilutions were made from this solution for the different inoculations. For disease inoculations, 4-week-old *Arabidopsis* plants (SD conditions) were syringe infiltrated with *Pst*DC3000 at 10⁵ colony-forming units (cfu) mL⁻¹ (OD₆₀₀=0.0002) in 10 mM MgCl₂ and 0.02% v/v silwet L77. Leaf disc samples from eight plants (*n* = 8) were taken directly after infiltration (*t*=0 d) and three days post infiltration (*t*=3 d). Leaf discs were macerated (Mixer Mill, Retsch) in 10 mM MgCl₂, serially diluted and plated for colony counting. Bacterial growth in the transgenic and *sum* knock-out lines was compared with that of the wild-type (*Col-0*). To assess the development of disease symptoms caused by *Pst* infection, plants were infiltrated with 5 \times 10⁶ cfu mL⁻¹ (OD₆₀₀=0.005) of *Pst*DC3000

and placed under a LD regime. In all cases, plants were placed under a translucent cover for 24 h prior to and post infection to increase humidity.

HR Assays (Ion Leakage and Trypan Blue Staining)

HR was examined using the ion leakage assay and trypan blue staining. HR was triggered by infiltrating *Pst*DC3000 carrying *avrRpm1* (hereafter, *Pst+avrRpm1*), which induces an RPM1-dependent HR in *Arabidopsis* (*Col-0*) within 7 h of infiltration (Dangl et al., 1992). For ion leakage assays, 4-week-old *Arabidopsis* plants (SD conditions) were infiltrated with *Pst+avrRpm1* at 5 \times 10⁷ cfu mL⁻¹ (OD₆₀₀ = 0.1) in 10 mM MgCl₂. Three leaf disc samples were taken from the infiltrated zones, extensively washed for 1 h in 50 mL water, and then placed in 3 mL water at ambient temperature with gyratory agitation. The conductivity was measured for 11 h per four leaf discs per genotype (B-173 conductivity meter; Horiba). Mean conductivity and SE were calculated for three repetitions per experiment. At least two additional independent transgenic lines were tested per construct. For trypan blue staining, 4-week-old *Arabidopsis* plants (SD conditions) were syringe infiltrated with *Pst+avrRpm1* (Grant et al., 1995) at 2.5 \times 10⁷ cfu mL⁻¹ (OD₆₀₀ = 0.05) in 10 mM MgCl₂. Seven hours after infiltration, the rosette leaves were stained with a 1:1 mixture (v/v) of ethanol and lactic acid–phenol–trypan blue solution (2.5 mg mL⁻¹ trypan blue, 25% [v/v] lactic acid, 25% phenol, 25% glycerol, and water) and boiled for 5 min. For destaining, the trypan blue solution was replaced with a chloral hydrate solution (2.5 g/mL in water).

RNA Analysis

Total RNA was extracted using Trizol reagent (Invitrogen) according to the manufacturer's recommendations. For cDNA synthesis, 2 μ g RNA was used in combination with Superscript III (Invitrogen). Real-time PCRs were performed in an ABI 7500 real-time PCR system (Applied Biosystems) using a Platinum SYBR Green qPCR SuperMix-UDG Kit (Invitrogen). The cycling program was set to 2 min, 50°C; 10 min, 95°C; 40 cycles of 15 s at 95°C; and 1 min, 60°C, and a melting curve analysis was performed at the end of the PCR. Primer pairs were tested for specificity and for amplification efficiency with a standard cDNA dilution curve. PCR amplification efficiencies were determined for each primer pair per plate using LinRegPCR, and the mean PCR amplification efficiency for each primer pair per plate was subsequently used to determine the gene expression levels for the different samples (Ruijter et al., 2009). The different biological samples were subsequently normalized against expression of β -Tubulin4 (TUB4). Quantitative expression analysis was conducted for at least three independent experiments including at least three independent biological replicates per sample in each experiment.

SA and flg22 Treatment

Four-week-old SD plants were placed in high humidity chambers for 24 h prior to treatment. Plants were spray inoculated with 1 mM SA in 0.015% (v/v) Silwet-L77 or mock treated (0.015% [v/v] Silwet-L77) and returned to high humidity. Active Flg22 peptide and inactive Flg22^{Atum} peptide were synthesized by Genscript and dissolved at 10 μ M prior to infiltration. Samples for RNA extraction were taken at the indicated time points, and cDNA was prepared as outlined above.

Protein Work

For α PR1 immunoblot analysis, seedlings were homogenized in liquid nitrogen, thawed on ice in extraction buffer (50 mM Tris-HCl, pH 7.5, 150 mM NaCl, 5 mM EDTA, 2% [w/v] polyvinylpyrrolidone K25, 1 \times protease inhibitors, 0.5% Nonidet P-40, and 2 mM DTT), and centrifuged for 10 min at 13,000g. The supernatant was mixed 1:1 with 2 \times SB (125 mM Tris-HCl, pH 6.8, 4% SDS, 20% glycerol, and 100 mM DTT), and the samples were

boiled for 10 min. Proteins were separated on 15% SDS-PAGE and blotted onto polyvinylidene fluoride membrane. Secondary immunoglobulins conjugated to horseradish peroxidase were visualized using ECL Plus (GE Healthcare). Primary antibodies against *Arabidopsis* SUM1/2, SUM3 (Abcam) (Kurepa et al., 2003), His-tag (α -pentaHis; Qiagen), and PR (α PR1; March-Diaz et al., 2008) are described elsewhere. For heat shock-induced hyper-SUMOylation, *Arabidopsis* seedlings were grown in liquid culture for 14 d under continuous light at 22°C, exposed to a 30-min heat shock at 37°C, and then returned to 22°C for 1 h (Kurepa et al., 2003). Total protein was extracted as described above (the extraction buffer included in addition 20 mM NEM and 8 M Urea) and separated on SDS-PAGE gradient gels (6 to 20%) for immunoblotting. For Ni²⁺ resin affinity precipitations, plant material was dissolved in extraction buffer that included 20 mM NEM and 6 M GuCl, and, after clarification, the protein samples were incubated with Ni²⁺ resin for 2 h at 4°C, followed by three washes of the resin with wash buffer (50 mM Tris-HCl, pH 7.5, 150 mM NaCl, 2 mM EDTA, 0.5% Nonidet P-40, and 8 M urea). The bound fraction was eluted by boiling in 1 × SB for 10 min and loaded on SDS-PAGE. The total protein fraction containing GuCl was precipitated with 10% (w/v) trichloroacetic acid and washed twice in ice-cold 80% acetone prior to loading on SDS-PAGE. The protein precipitate was redissolved in 1 × SB prior to loading.

Phylogeny

Phylogenetic analyses were conducted in MEGA4 using Minimum Evolution. The percentage of replicate trees in which the associated taxa clustered together in the bootstrap test (1000 replicates) is shown next to the branches. Taxa that were supported by <50% of the replicates are collapsed. There were a total of 80 positions in the final data set. The ME tree was searched using the Close-Neighbor-Interchange algorithm at a search level of 3. The neighbor-joining algorithm was used to generate the initial tree. All positions containing gaps and missing data were eliminated from the data set (complete deletion option).

Accession Numbers

Sequence data from this article can be found in the Arabidopsis Genome Initiative under the following identifiers: SUM1 (At4g25600), SUM2 (At5g55160), SUM3 (At5g55170), SIZ1 (At5G60410), ESD4 (At4G15880), OTS1 (At1g60220), OTS2 (At1g10570), ICS1 (At1G74710), PR1 (At2g14610), and TUB4 (At5g44340).

Supplemental Data

The following materials are available in the online version of this article.

Supplemental Figure 1. Phylogeny Analysis of the SUMO Gene Family.

Supplemental Figure 2. Localization of β -Glucuronidase (GUS) Reporter Activity in *Arabidopsis* Plants Transformed with *ProSUM1-GUS* (S1) or *ProSUM2-GUS* (S2) during *Arabidopsis* Embryogenesis.

Supplemental Figure 3. HN-Tagged SUMO Is Rapidly Deconjugated in the Absence of the SUMO Protease Inhibitor NEM in Plant Protein Extracts.

Supplemental Figure 4. Overexpression of SUMO Variants Resulted in eEarly Flowering under SD Conditions.

Supplemental Figure 5. Overexpression of SUM3 Variants Did Not Influence Overall SUM1/2 Conjugation Levels in Planta.

Supplemental Figure 6. Relative Expression Levels of the Transgene Encoding HN-Tagged SUM3 in Comparison to the Expression Levels of the Endogenous *SUM3* Gene.

Supplemental Figure 7. Quantitative Analysis of AvrRpm1-Mediated HR Induction in *Arabidopsis* Plants Overexpressing SUMO Variants using Trypan Blue Staining.

Supplemental Figure 8. Overexpressing SUMO Variants in *Arabidopsis* Results in Spontaneous Cell Death Similar to the *siz1* Mutant.

Supplemental Figure 9. Treatment with SA of *Arabidopsis* Overexpressing SUM3 Variants Result in a Unknown Modification of HN-Tagged SUM3 without Affecting the Overall SUM3 Conjugation Levels to Other Proteins.

Supplemental Figure 10. Plants Overexpressing His-Tagged SUM1 Show Enhanced Expression of the SA Marker Gene *PR1*.

Supplemental Table 1. Overexpression of SUMO Variants Resulted in Early Flowering under SD Conditions.

Supplemental Data Set 1. Protein Sequences Used to Generate the Phylogeny Presented in Supplemental Figure 1.

ACKNOWLEDGMENTS

We thank S.v. Wees, R. Vierstra, J.C. Reyes, N.H. Chua, and G. Coupland for providing seeds and/or specific antibodies. LinRegPCR was kindly provided by J.M. Ruijter. We kindly acknowledge D. Weigel for providing pRS300 and S. Ossowski for help with design of amiRNAs. We thank H. Lemereis and L. Tikovsky for plant care and P. van Egmond for assisting with SA measurements. H.A.V.D.B. was supported by Netherlands Organisation for Scientific Research (NWO)-VENI Grant 863.04.018. R.K.K. was supported by BOYSCAST Fellowship, Department of Science and Technology, Government of India. Work in the Takken lab is supported in part by grants from the Netherlands Genomics Initiative (CBSG2012) and the European Union framework 6 program Bioexploit and in the Schuurink lab by NWO Grant 818.02.017.

Received August 25, 2009; revised April 28, 2010; accepted May 13, 2010; published June 4, 2010.

REFERENCES

- Ankar, J., and Sistonen, L. (2007). SUMO: Getting it on. *Biochem. Soc. Trans.* **35**: 1409–1413.
- Baurle, I., and Dean, C. (2006). The timing of developmental transitions in plants. *Cell* **125**: 655–664.
- Bernier-Villamor, V., Sampson, D.A., Matunis, M.J., and Lima, C.D. (2002). Structural basis for E2-mediated SUMO conjugation revealed by a complex between ubiquitin-conjugating enzyme Ubc9 and RanGAP1. *Cell* **108**: 345–356.
- Birnbaum, K., Shasha, D.E., Wang, J.Y., Jung, J.W., Lambert, G.M., Galbraith, D.W., and Benfey, P.N. (2003). A gene expression map of the *Arabidopsis* root. *Science* **302**: 1956–1960.
- Blomster, H.A., Hietakangas, V., Wu, J., Kouvonen, P., Hautaniemi, S., and Sistonen, L. (2009). Novel proteomics strategy brings insight into the prevalence of SUMO-2 target sites. *Mol. Cell. Proteomics* **8**: 1382–1390.
- Brady, S.M., Orlando, D.A., Lee, J.Y., Wang, J.Y., Koch, J., Dinneny, J.R., Mace, D., Ohler, U., and Benfey, P.N. (2007). A high-resolution root spatiotemporal map reveals dominant expression patterns. *Science* **318**: 801–806.
- Budhiraja, R., Hermkes, R., Muller, S., Schmidt, J., Colby, T., Panigrahi, K., Coupland, G., and Bachmair, A. (2009). Substrates related to chromatin and to RNA-dependent processes are modified

- by *Arabidopsis* SUMO isoforms that differ in a conserved residue with influence on desumoylation. *Plant Physiol.* **149**: 1529–1540.
- Casson, S., Spencer, M., Walker, K., and Lindsey, K.** (2005). Laser capture microdissection for the analysis of gene expression during embryogenesis of *Arabidopsis*. *Plant J.* **42**: 111–123.
- Catala, R., Ouyang, J., Abreu, I.A., Hu, Y., Seo, H., Zhang, X., and Chua, N.H.** (2007). The *Arabidopsis* E3 SUMO ligase SIZ1 regulates plant growth and drought responses. *Plant Cell* **19**: 2952–2966.
- Cheong, M.S., Park, H.C., Hong, M.J., Lee, J., Choi, W., Jin, J.B., Bohnert, H.J., Lee, S.Y., Bressan, R.A., and Yun, D.J.** (2009). Specific domain structures control abscisic acid-, salicylic acid-, and stress-mediated SIZ1 phenotypes. *Plant Physiol.* **151**: 1930–1942.
- Chosed, R., Mukherjee, S., Lois, L.M., and Orth, K.** (2006). Evolution of a signalling system that incorporates both redundancy and diversity: *Arabidopsis* SUMOylation. *Biochem. J.* **398**: 521–529.
- Clough, S.J., and Bent, A.F.** (1998). Floral dip: A simplified method for *Agrobacterium*-mediated transformation of *Arabidopsis thaliana*. *Plant J.* **16**: 735–743.
- Colby, T., Matthai, A., Boeckelmann, A., and Stuible, H.P.** (2006). SUMO-conjugating and SUMO-deconjugating enzymes from *Arabidopsis*. *Plant Physiol.* **142**: 318–332.
- Conti, L., Price, G., O'Donnell, E., Schwessinger, B., Dominy, P., and Sadanandom, A.** (2008). Small ubiquitin-like modifier proteases OVERLY TOLERANT TO SALT1 and -2 regulate salt stress responses in *Arabidopsis*. *Plant Cell* **20**: 2894–2908.
- Custers, J.B.M., Snepvangers, S.C.H.J., Jansen, H.J., Zhang, L., and van Lookeren Campagne, M.M.** (1999). The 35S-CaMV promoter is silent during early embryogenesis but activated during nonembryogenic sporophytic development in microspore culture. *Protoplasma* **208**: 257–264.
- Dangl, J.L., Ritter, C., Gibbon, M.J., Mur, L.A., Wood, J.R., Goss, S., Mansfield, J., Taylor, J.D., and Vivian, A.** (1992). Functional homologs of the *Arabidopsis* RPM1 disease resistance gene in bean and pea. *Plant Cell* **4**: 1359–1369.
- Devadas, S.K., and Raina, R.** (2002). Preexisting systemic acquired resistance suppresses hypersensitive response-associated cell death in *Arabidopsis* hr11 mutant. *Plant Physiol.* **128**: 1234–1244.
- Diesel, C., von Dahl, C.C., Gaquerel, E., and Baldwin, I.T.** (2009). Different lepidopteran elicitors account for cross-talk in herbivory-induced phytohormone signaling. *Plant Physiol.* **150**: 1576–1586.
- Downes, B., and Vierstra, R.D.** (2005). Post-translational regulation in plants employing a diverse set of polypeptide tags. *Biochem. Soc. Trans.* **33**: 393–399.
- Garcia-Dominguez, M., March-Diaz, R., and Reyes, J.C.** (2008). The PHD domain of plant PIAS proteins mediates sumoylation of bromodomain GTE proteins. *J. Biol. Chem.* **283**: 21469–21477.
- Garcion, C., Lohmann, A., Lamodiere, E., Catinot, J., Buchala, A., Doermann, P., and Metraux, J.P.** (2008). Characterization and biological function of the ISOCHORISMATE SYNTHASE2 gene of *Arabidopsis*. *Plant Physiol.* **147**: 1279–1287.
- Ghisletti, S., Huang, W., Ogawa, S., Pascual, G., Lin, M.E., Willson, T.M., Rosenfeld, M.G., and Glass, C.K.** (2007). Parallel SUMOylation-dependent pathways mediate gene- and signal-specific transcription repression by LXRs and PPARgamma. *Mol. Cell* **25**: 57–70.
- Grant, M.R., Godiard, L., Straube, E., Ashfield, T., Lewald, J., Sattler, A., Innes, R.W., and Dangl, J.L.** (1995). Structure of the *Arabidopsis* RPM1 gene enabling dual specificity disease resistance. *Science* **269**: 843–846.
- Hecker, C.M., Rabiller, M., Haglund, K., Bayer, P., and Dikic, I.** (2006). Specification of SUMO1- and SUMO2-interacting motifs. *J. Biol. Chem.* **281**: 16117–16127.
- Heil, M., and Baldwin, I.T.** (2002). Fitness costs of induced resistance: Emerging experimental support for a slippery concept. *Trends Plant Sci.* **7**: 61–67.
- Heun, P.** (2007). SUMO organization of the nucleus. *Curr. Opin. Cell Biol.* **19**: 350–355.
- Hotson, A., Chosed, R., Shu, H., Orth, K., and Mudgett, M.B.** (2003). *Xanthomonas* type III effector XopD targets SUMO-conjugated proteins in planta. *Mol. Microbiol.* **50**: 377–389.
- Huang, L., Yang, S., Zhang, S., Liu, M., Lai, J., Qi, Y., Shi, S., Wang, J., Wang, Y., Xie, Q., and Yang, C.** (2009). The *Arabidopsis* SUMO E3 ligase AtMMS21, a homologue of NSE2/MMS21, regulates cell proliferation in the root. *Plant J.* **60**: 666–678.
- Ihara, M., Koyama, H., Uchimura, Y., Saitoh, H., and Kikuchi, A.** (2007). Noncovalent binding of small ubiquitin-related modifier (SUMO) protease to SUMO is necessary for enzymatic activities and cell growth. *J. Biol. Chem.* **282**: 16465–16475.
- Ishida, T., Fujiwara, S., Miura, K., Stacey, N., Yoshimura, M., Schneider, K., Adachi, S., Minamisawa, K., Umeda, M., and Sugimoto, K.** (2009). SUMO E3 Ligase HIGH PLOIDY2 regulates endocycle onset and meristem maintenance in *Arabidopsis*. *Plant Cell* **21**: 2284–2297.
- Jefferson, R.A., Kavanagh, T.A., and Bevan, M.W.** (1987). GUS fusions: Beta-glucuronidase as a sensitive and versatile gene fusion marker in higher plants. *EMBO J.* **6**: 3901–3907.
- Jin, J.B., et al.** (2008). The SUMO E3 ligase, AtSIZ1, regulates flowering by controlling a salicylic acid-mediated floral promotion pathway and through affects on FLC chromatin structure. *Plant J.* **53**: 530–540.
- Journot-Catalino, N., Somssich, I.E., Roby, D., and Kroj, T.** (2006). The transcription factors WRKY11 and WRKY17 act as negative regulators of basal resistance in *Arabidopsis thaliana*. *Plant Cell* **18**: 3289–3302.
- Kim, J.G., Taylor, K.W., Hotson, A., Keegan, M., Schmelz, E.A., and Mudgett, M.B.** (2008). XopD SUMO protease affects host transcription, promotes pathogen growth, and delays symptom development in *Xanthomonas*-infected tomato leaves. *Plant Cell* **20**: 1915–1929.
- Knipscheer, P., Flotho, A., Klug, H., Olsen, J.V., van Dijk, W.J., Fish, A., Johnson, E.S., Mann, M., Sixma, T.K., and Pichler, A.** (2008). Ubc9 sumoylation regulates SUMO target discrimination. *Mol. Cell* **31**: 371–382.
- Kurepa, J., Walker, J.M., Smalle, J., Gosink, M.M., Davis, S.J., Durham, T.L., Sung, D.Y., and Vierstra, R.D.** (2003). The small ubiquitin-like modifier (SUMO) protein modification system in *Arabidopsis*. Accumulation of SUMO1 and -2 conjugates is increased by stress. *J. Biol. Chem.* **278**: 6862–6872.
- Lamla, T., and Erdmann, V.A.** (2004). The Nano-tag, a streptavidin-binding peptide for the purification and detection of recombinant proteins. *Protein Expr. Purif.* **33**: 39–47.
- Lee, J., et al.** (2007). Salicylic acid-mediated innate immunity in *Arabidopsis* is regulated by SIZ1 SUMO E3 ligase. *Plant J.* **49**: 79–90.
- Lois, L.M., Lima, C.D., and Chua, N.H.** (2003). Small ubiquitin-like modifier modulates abscisic acid signaling in *Arabidopsis*. *Plant Cell* **15**: 1347–1359.
- Lorrain, S., Vaillieu, F., Balague, C., and Roby, D.** (2003). Lesion mimic mutants: Keys for deciphering cell death and defense pathways in plants? *Trends Plant Sci.* **8**: 263–271.
- March-Diaz, R., Garcia-Dominguez, M., Lozano-Juste, J., Leon, J., Florencio, F.J., and Reyes, J.C.** (2008). Histone H2A.Z and homologues of components of the SWR1 complex are required to control immunity in *Arabidopsis*. *Plant J.* **53**: 475–487.
- Martinez, C., Pons, E., Prats, G., and Leon, J.** (2004). Salicylic acid regulates flowering time and links defence responses and reproductive development. *Plant J.* **37**: 209–217.

- Matic, I., Macek, B., Hilger, M., Walther, T.C., and Mann, M.** (2008). Phosphorylation of SUMO-1 occurs in vivo and is conserved through evolution. *J. Proteome Res.* **7**: 4050–4057.
- Meulmeester, E., Kunze, M., Hsiao, H.H., Urlaub, H., and Melchior, F.** (2008). Mechanism and consequences for paralog-specific sumoylation of ubiquitin-specific protease 25. *Mol. Cell* **30**: 610–619.
- Miura, K., Jin, J.B., and Hasegawa, P.M.** (2007a). Sumoylation, a post-translational regulatory process in plants. *Curr. Opin. Plant Biol.* **10**: 495–502.
- Miura, K., Jin, J.B., Lee, J., Yoo, C.Y., Stirn, V., Miura, T., Ashworth, E.N., Bressan, R.A., Yun, D.J., and Hasegawa, P.M.** (2007b). SIZ1-mediated sumoylation of ICE1 controls CBF3/DREB1A expression and freezing tolerance in *Arabidopsis*. *Plant Cell* **19**: 1403–1414.
- Miura, K., Lee, J., Jin, J.B., Yoo, C.Y., Miura, T., and Hasegawa, P.M.** (2009). Sumoylation of ABI5 by the *Arabidopsis* SUMO E3 ligase SIZ1 negatively regulates abscisic acid signaling. *Proc. Natl. Acad. Sci. USA* **106**: 5418–5423.
- Miura, K., Lee, J., Miura, T., and Hasegawa, P.M.** (2010). SIZ1 controls cell growth and plant development in *Arabidopsis* through salicylic acid. *Plant Cell Physiol.* **51**: 103–113.
- Miura, K., Rus, A., Sharkhuu, A., Yokoi, S., Karthikeyan, A.S., Raghothama, K.G., Baek, D., Koo, Y.D., Jin, J.B., Bressan, R.A., Yun, D.J., and Hasegawa, P.M.** (2005). The *Arabidopsis* SUMO E3 ligase SIZ1 controls phosphate deficiency responses. *Proc. Natl. Acad. Sci. USA* **102**: 7760–7765.
- Mukhopadhyay, D., and Dasso, M.** (2007). Modification in reverse: the SUMO proteases. *Trends Biochem. Sci.* **32**: 286–295.
- Murtas, G., Reeves, P.H., Fu, Y.F., Bancroft, I., Dean, C., and Coupland, G.** (2003). A nuclear protease required for flowering-time regulation in *Arabidopsis* reduces the abundance of SMALL UBIQUITIN-RELATED MODIFIER conjugates. *Plant Cell* **15**: 2308–2319.
- Novatchkova, M., Budhiraja, R., Coupland, G., Eisenhaber, F., and Bachmair, A.** (2004). SUMO conjugation in plants. *Planta* **220**: 1–8.
- Rate, D.N., and Greenberg, J.T.** (2001). The *Arabidopsis* aberrant growth and death2 mutant shows resistance to *Pseudomonas syringae* and reveals a role for NPR1 in suppressing hypersensitive cell death. *Plant J.* **27**: 203–211.
- Reeves, P.H., Murtas, G., Dash, S., and Coupland, G.** (2002). early in short days 4, a mutation in *Arabidopsis* that causes early flowering and reduces the mRNA abundance of the floral repressor FLC. *Development* **129**: 5349–5361.
- Reindle, A., Belichenko, I., Bylebyl, G.R., Chen, X.L., Gandhi, N., and Johnson, E.S.** (2006). Multiple domains in Siz SUMO ligases contribute to substrate selectivity. *J. Cell Sci.* **119**: 4749–4757.
- Ruijter, J.M., Ramakers, C., Hoogaars, W.M., Karlen, Y., Bakker, O., van den Hoff, M.J., and Moorman, A.F.** (2009). Amplification efficiency: Linking baseline and bias in the analysis of quantitative PCR data. *Nucleic Acids Res.* **37**: e45.
- Rytinki, M.M., Kaikkonen, S., Pehkonen, P., Jaaskelainen, T., and Palvimo, J.J.** (2009). PIAS proteins: Pleiotropic interactors associated with SUMO. *Cell. Mol. Life Sci.* **66**: 3029–3041.
- Saracco, S.A., Miller, M.J., Kurepa, J., and Vierstra, R.D.** (2007). Genetic analysis of SUMOylation in *Arabidopsis*: conjugation of SUMO1 and SUMO2 to nuclear proteins is essential. *Plant Physiol.* **145**: 119–134.
- Schwab, R., Ossowski, S., Riester, M., Warthmann, N., and Weigel, D.** (2006). Highly specific gene silencing by artificial microRNAs in *Arabidopsis*. *Plant Cell* **18**: 1121–1133.
- Shapiro, A.D., and Zhang, C.** (2001). The role of NDR1 in avirulence gene-directed signaling and control of programmed cell death in *Arabidopsis*. *Plant Physiol.* **127**: 1089–1101.
- Shen, L., Tatham, M.H., Dong, C., Zagorska, A., Naismith, J.H., and Hay, R.T.** (2006). SUMO protease SENP1 induces isomerization of the scissile peptide bond. *Nat. Struct. Mol. Biol.* **13**: 1069–1077.
- Strawn, M.A., Marr, S.K., Inoue, K., Inada, N., Zubieta, C., and Wildermuth, M.C.** (2007). *Arabidopsis* isochorismate synthase functional in pathogen-induced salicylate biosynthesis exhibits properties consistent with a role in diverse stress responses. *J. Biol. Chem.* **282**: 5919–5933.
- Sunilkumar, G., Mohr, L., Lopata-Finch, E., Emani, C., and Rathore, K.S.** (2002). Developmental and tissue-specific expression of CaMV 35S promoter in cotton as revealed by GFP. *Plant Mol. Biol.* **50**: 463–474.
- Thibaud-Nissen, F., Wu, H., Richmond, T., Redman, J.C., Johnson, C., Green, R., Arias, J., and Town, C.D.** (2006). Development of *Arabidopsis* whole-genome microarrays and their application to the discovery of binding sites for the TGA2 transcription factor in salicylic acid-treated plants. *Plant J.* **47**: 152–162.
- Thilmony, R., Underwood, W., and He, S.Y.** (2006). Genome-wide transcriptional analysis of the *Arabidopsis thaliana* interaction with the plant pathogen *Pseudomonas syringae* pv. *tomato* DC3000 and the human pathogen *Escherichia coli* O157:H7. *Plant J.* **46**: 34–53.
- Tissier, A.F., Marillonnet, S., Klimyuk, V., Patel, K., Torres, M.A., Murphy, G., and Jones, J.D.** (1999). Multiple independent defective suppressor-mutator transposon insertions in *Arabidopsis*: A tool for functional genomics. *Plant Cell* **11**: 1841–1852.
- Underwood, W., Zhang, S., and He, S.Y.** (2007). The *Pseudomonas syringae* type III effector tyrosine phosphatase HopAO1 suppresses innate immunity in *Arabidopsis thaliana*. *Plant J.* **52**: 658–672.
- van den Burg, H.A., and Takken, F.L.W.** (2009). Does chromatin remodeling mark systemic acquired resistance? *Trends Plant Sci.* **14**: 286–294.
- Verberne, M.C., Brouwer, N., Delbianco, F., Linthorst, H.J., Bol, J.F., and Verpoorte, R.** (2002). Method for the extraction of the volatile compound salicylic acid from tobacco leaf material. *Phytochem. Anal.* **13**: 45–50.
- Wang, D., Amornsiripanitch, N., and Dong, X.** (2006). A genomic approach to identify regulatory nodes in the transcriptional network of systemic acquired resistance in plants. *PLoS Pathog.* **2**: e123.
- Wildermuth, M.C., Dewdney, J., Wu, G., and Ausubel, F.M.** (2001). Isochorismate synthase is required to synthesize salicylic acid for plant defence. *Nature* **414**: 562–565.
- Winter, D., Vinegar, B., Nahal, H., Ammar, R., Wilson, G.V., and Provart, N.J.** (2007). An “electronic fluorescent pictograph” browser for exploring and analyzing large-scale biological data sets. *PLoS One* **2**: e718.
- Wohlschlegel, J.A., Johnson, E.S., Reed, S.I., and Yates III, J.R.** (2004). Global analysis of protein sumoylation in *Saccharomyces cerevisiae*. *J. Biol. Chem.* **279**: 45662–45668.
- Xu, X.M., Rose, A., Muthuswamy, S., Jeong, S.Y., Venkatakrishnan, S., Zhao, Q., and Meier, I.** (2007). NUCLEAR PORE ANCHOR, the *Arabidopsis* homolog of Tpr/Mlp1/Mlp2/megator, is involved in mRNA export and SUMO homeostasis and affects diverse aspects of plant development. *Plant Cell* **19**: 1537–1548.
- Yaeno, T., and Iba, K.** (2008). BAH1/NLA, a RING-type ubiquitin E3 ligase, regulates the accumulation of salicylic acid and immune responses to *Pseudomonas syringae* DC3000. *Plant Physiol.* **148**: 1032–1041.
- Yamaguchi, T., Sharma, P., Athanasiou, M., Kumar, A., Yamada, S., and Kuehn, M.R.** (2005). Mutation of SENP1/SuPr-2 reveals an essential role for desumoylation in mouse development. *Mol. Cell. Biol.* **25**: 5171–5182.
- Yoo, C.Y., Miura, K., Jin, J.B., Lee, J., Park, H.C., Salt, D.E., Yun,**

- D.J., Bressan, R.A., and Hasegawa, P.M.** (2006). SIZ1 small ubiquitin-like modifier E3 ligase facilitates basal thermotolerance in *Arabidopsis* independent of salicylic acid. *Plant Physiol.* **142**: 1548–1558.
- Yunus, A.A., and Lima, C.D.** (2006). Lysine activation and functional analysis of E2-mediated conjugation in the SUMO pathway. *Nat. Struct. Mol. Biol.* **13**: 491–499.
- Zhu, J., Zhu, S., Guzzo, C.M., Ellis, N.A., Sung, K.S., Choi, C.Y., and Matunis, M.J.** (2008). Small ubiquitin-related modifier (SUMO) binding determines substrate recognition and paralog-selective SUMO modification. *J. Biol. Chem.* **283**: 29405–29415.
- Zhu, S., Goeres, J., Sixt, K.M., Bekes, M., Zhang, X.D., Salvesen, G.S., and Matunis, M.J.** (2009). Protection from isopeptidase-mediated deconjugation regulates paralog-selective sumoylation of RanGAP1. *Mol. Cell* **33**: 570–580.
- Zipfel, C., Robatzek, S., Navarro, L., Oakeley, E.J., Jones, J.D., Felix, G., and Boller, T.** (2004). Bacterial disease resistance in *Arabidopsis* through flagellin perception. *Nature* **428**: 764–767.